Solar Wind Magnetosphere Coupling

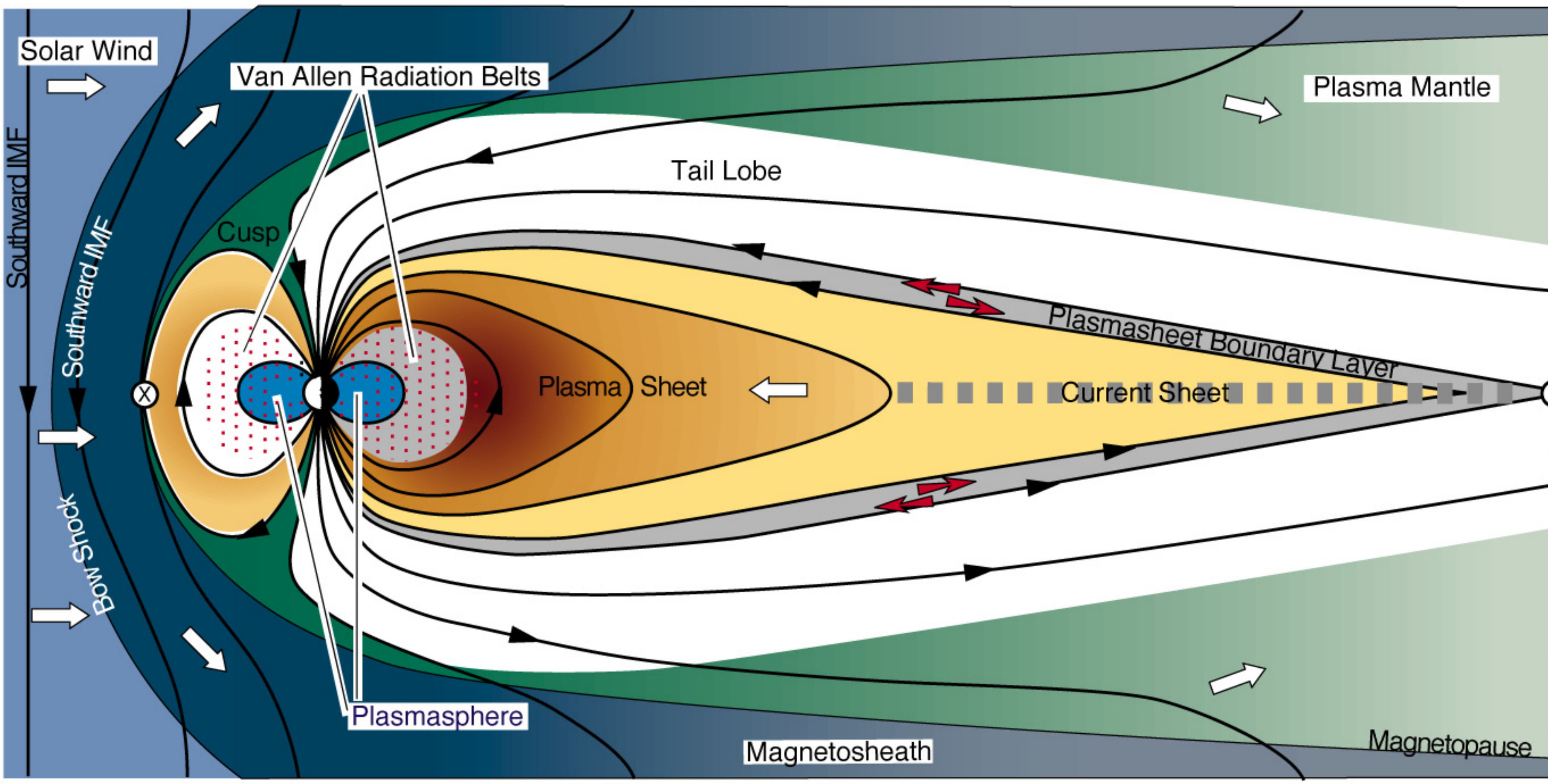

Figure courtesy T. W. Hill

F. Toffoletto, Rice University

with thanks to

R. A. Wolf and T. W. Hill, Rice U.

Outline

- Introduction
- Properties of the Solar Wind Near Earth
- The Magnetosheath
- The Magnetopause
- Basic Physical Processes that control Solar Wind Magnetosphere Coupling
  - Open and Closed Magnetosphere Processes
  - Electrodynamic coupling
  - Mass, Momentum and Energy coupling
  - The role of the ionosphere
- Current Status and Summary

QuickTime™ and a
YUV420 codec decompressor
are needed to see this picture.

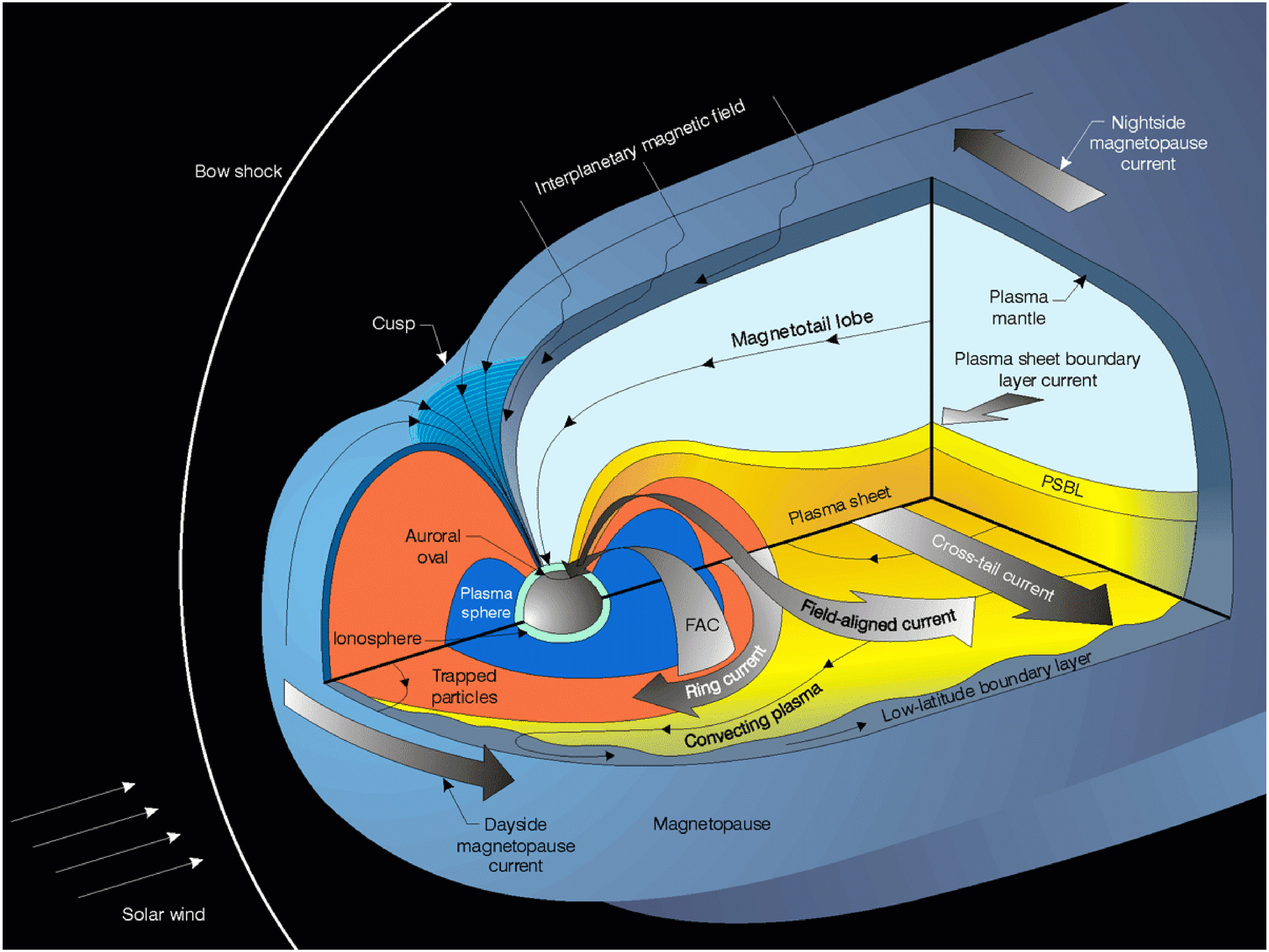

Bow shock
Interplanetary magnetic field
Nightside magnetopause current
Cusp
Plasma mantle
Magnetotail lobe
Plasma sheet boundary layer current
PSBL
Plasma sheet
Auroral oval
Cross-tail current
Plasma sphere
FAC
Field-aligned current
Ionosphere
Ring current
Trapped particles
Convecting plasma
Low-latitude boundary layer
Dayside magnetopause current
Magnetopause
Solar wind

Introduction

- By virtue of our proximity, the Earth's magnetosphere is the most studied and perhaps best understood magnetosphere
  - The system is rather complex in its structure and behavior and there are still some basic unresolved questions
  - Today's lecture will focus on describing the coupling to the major driver of the magnetosphere - the solar wind, and the ionosphere
  - Monday's lecture will look more at the more dynamic (and controversial) aspect of magnetospheric dynamics: storms and substorms

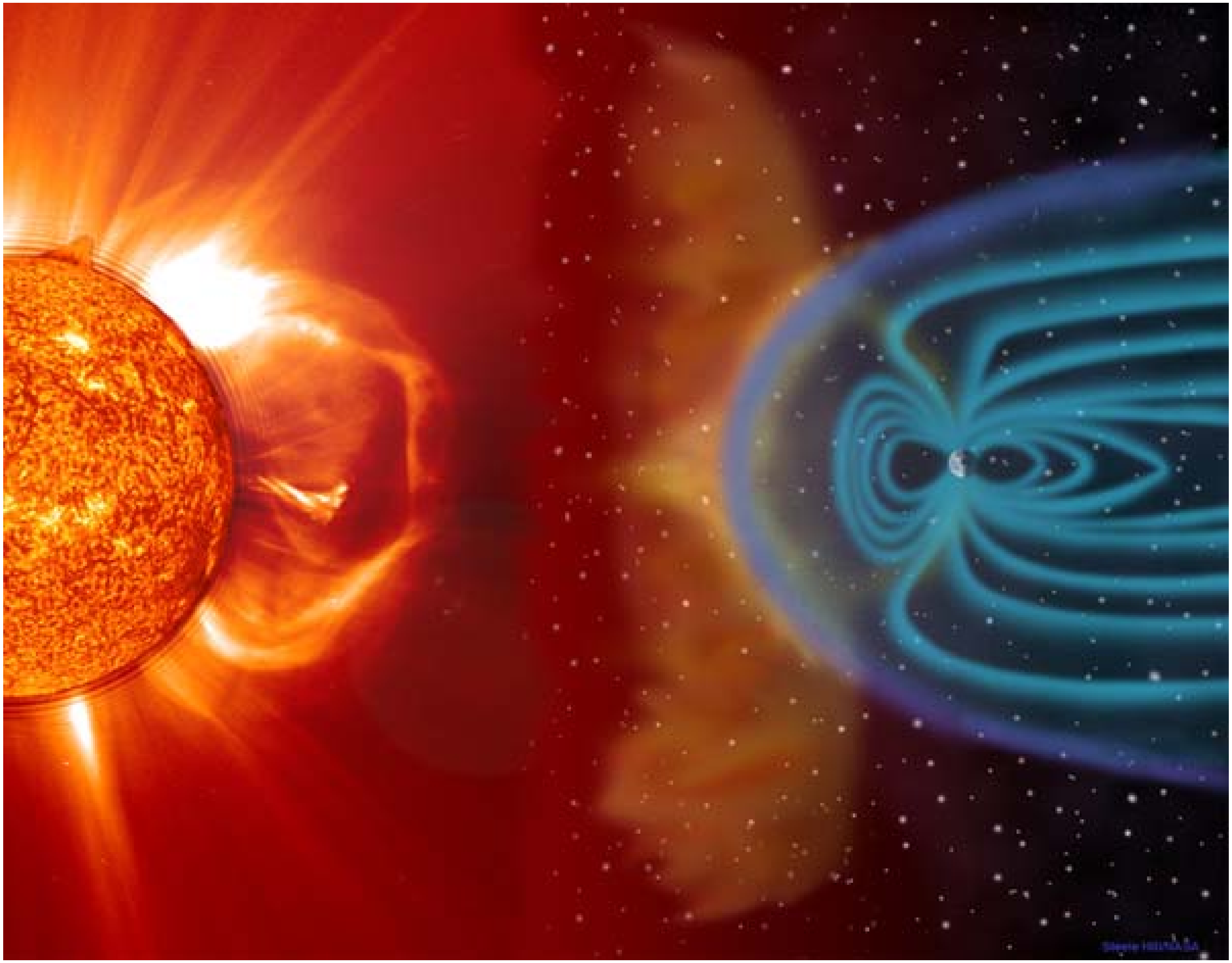

The Solar Wind Near the Earth

Solar-Wind Properties Observed Near Earth

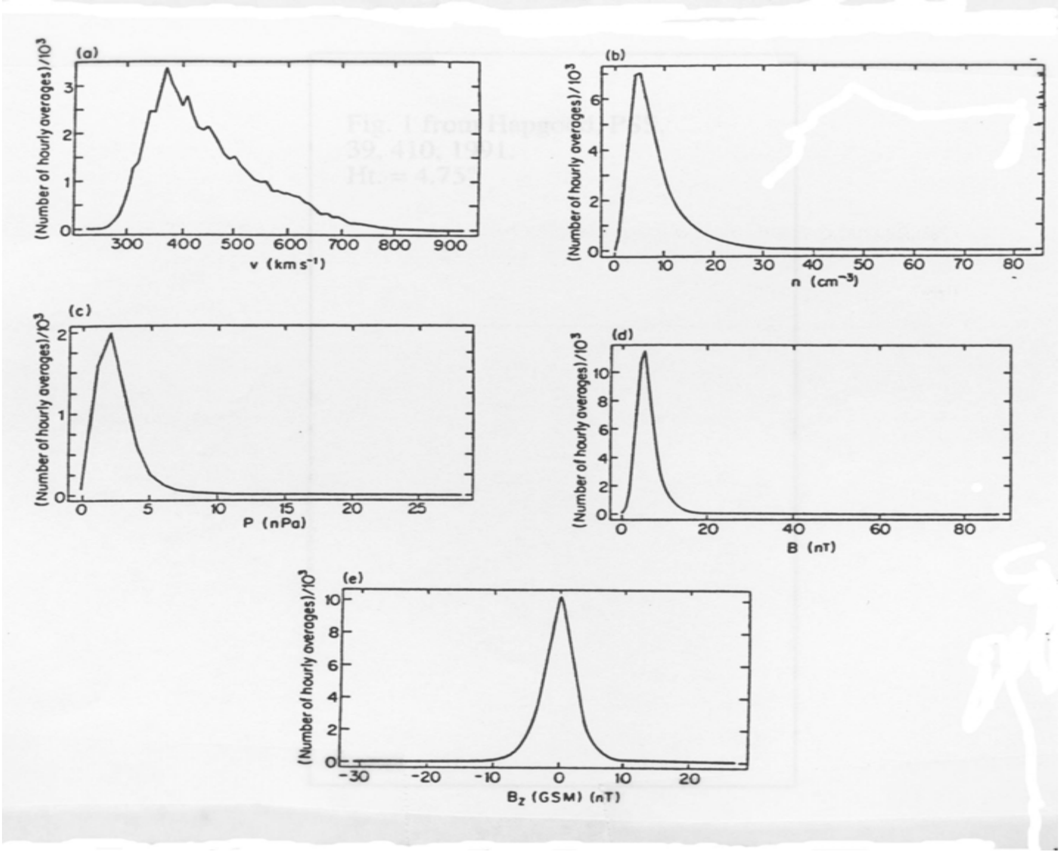

- Solar wind parameters observed by many spacecraft over period 1963-86. From Hapgood et al. (Planet. Space Sci., 39, 410, 1991).

Solar Wind Observed Near Earth

Values of Solar-Wind Parameters

Parameter	Minimum	Most Probable	Maximum
Velocity v (km/s)	250	370	2000×
Number density n (cm^{-3})		6	83
Ram pressure rv^2 (nPa)*		3	28
Magnetic field strength B (nanoteslas)	0	6	85
IMF B_z (nanoteslas)	-31	0¤	27

* 1 nPa = 1 nanoPascal = 10^{-9} Newtons/m^2.
Indicates at least one interval with $B < 0.1$ nT.
¤ Mean value was 0.014 nT, with a standard deviation of 3.3 nT.
× From Cliver *et al.*, *J. Geophys. Res.*, *95*, 17103, 1990. Measurements of high velocities in the Hapgood study were limited by instrumental effects.

From Feldman et al. (Solar Output and its Variations, Colorado Assoc. Univ. Press, 1977)

$$\langle T_p \rangle \sim 1.2\times10^{5}\,^{\circ}\mathrm{K} \quad \langle T_e \rangle \sim 1.4\times10^{5}\,^{\circ}\mathrm{K} \quad \langle T_e/T_p \rangle \sim 1.6$$

Solar Wind Observed Near Earth

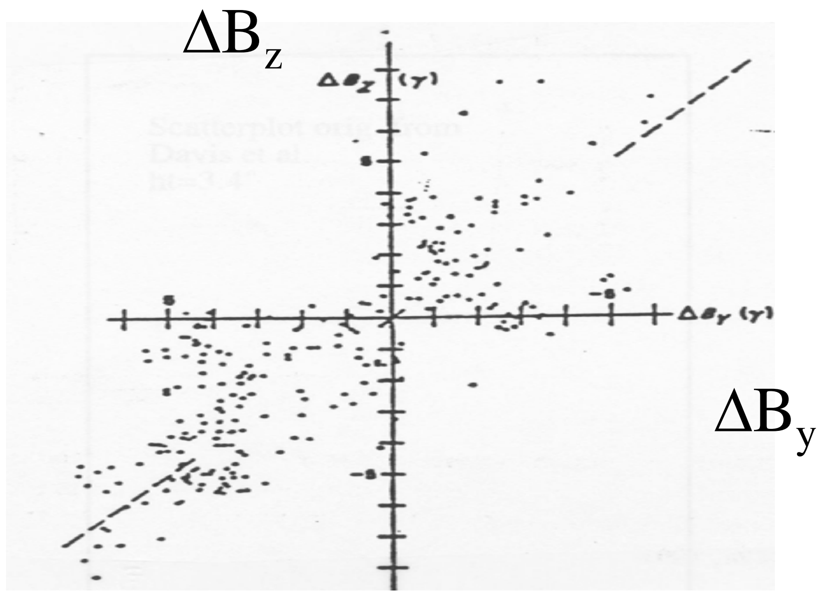

- Observed near Earth, the interplanetary magnetic field tends to make ~ 45˚ or ~225˚ angle with Sun-Earth direction.
  - Parker spiral.
- The north-south component of the IMF averages near zero and fluctuates on short time scales

Solar-Cycle Variation of Solar Wind Near Earth

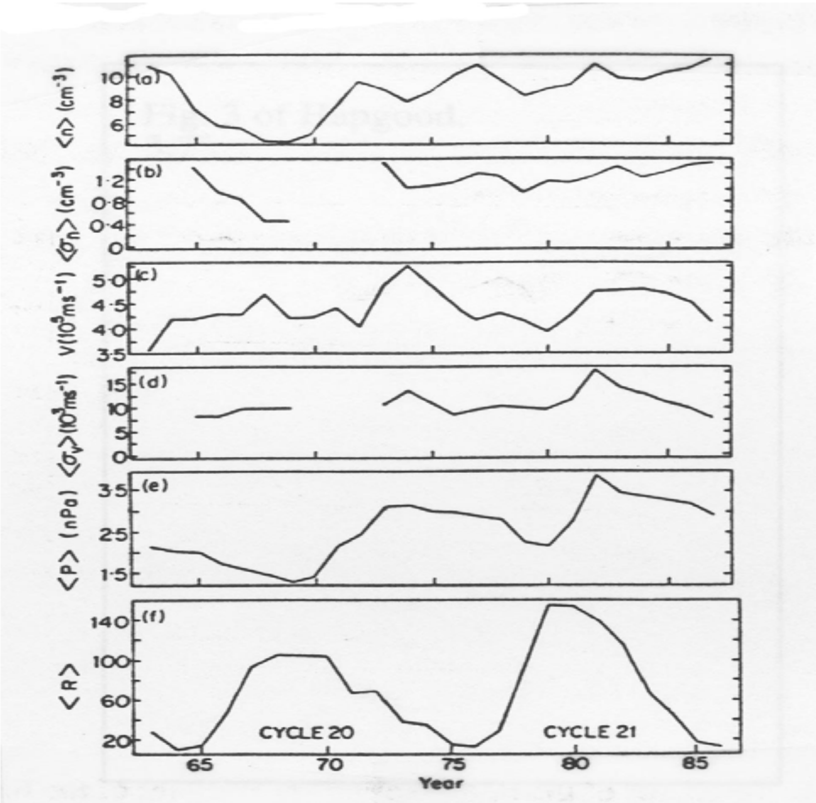

From Hapgood et al.(1991)

- Average velocity highest in declining phase of solar cycle.
- Successive solar cycles represent different polarities of Sun’s magnetic field.
- Magnetic-field reversal occurs near solar maximum.

Solar-Cycle Variation of Solar Wind Near Earth

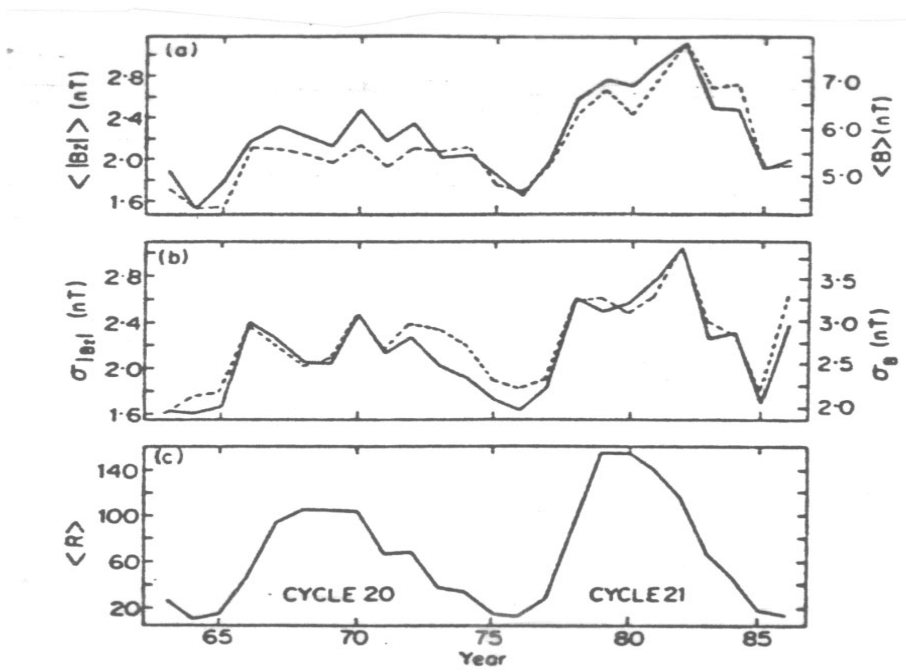

- Plot shows average absolute value of north-south IMF component.
- Highest near solar maximum.

Magnetosheath

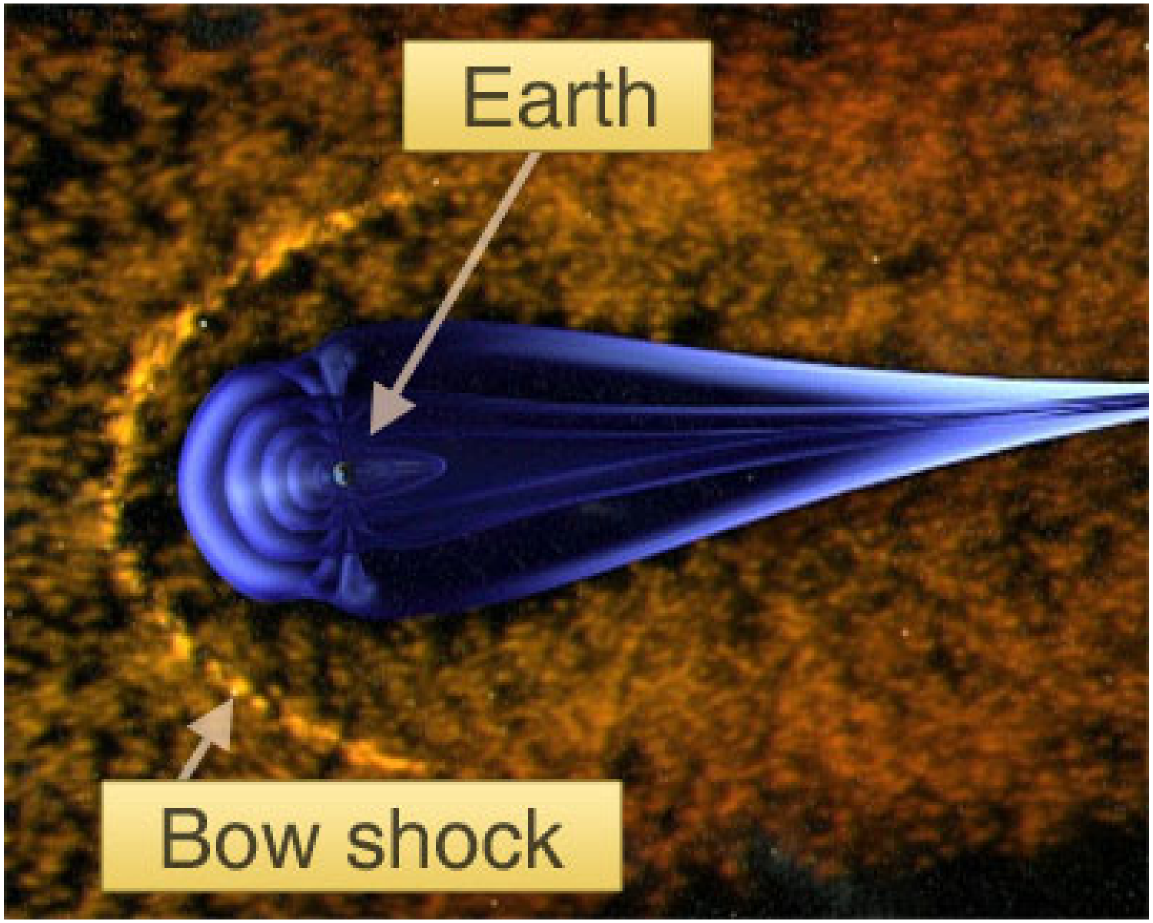

ESA

Question

- The energy of the solar wind has 3 components:
  - Thermal
  - Magnetic
  - Flow
- Which has the largest energy density?

Energy Densities in Solar Wind Near Earth

$$\left(\frac{1}{2}\rho v^2\right)_{sw} \approx \frac{1}{2}\left(1.67\times10^{-27}kg\right)\left(6cm^{-3}\right)(370km/s)^2 \approx 7\times10^{-10}J/m^3$$

$$\left\langle\frac{B^2}{2\mu_o}\right\rangle \approx \frac{(6nT)^2}{8\pi\times10^{-7}} \approx 1.4\times10^{-11}Jm^{-3} \sim 0.02\left(\frac{1}{2}\right)\rho v^2$$

$$\left\langle\frac{3}{2}nk(T_e+T_i)\right\rangle \approx \frac{3}{2}(6cm^{-3})(1.38\times10^{-23})(1.2+1.4)10^5 \sim 3\times10^{-11}J/m^3$$

$$\rho v^2 >> p \;\; or \;\; \frac{B^2}{2\mu_o}$$

$$\langle M_A\rangle = \left\langle\frac{v}{\sqrt{\frac{B^2}{\mu_o\rho}}}\right\rangle \sim 7 \qquad \langle M_S\rangle = \left\langle\frac{v}{\sqrt{\frac{5p}{3\rho}}}\right\rangle \sim 8$$

- Flow controls the magnetic field, drags it along.
  - Magnetic field is essentially frozen to the plasma

Magnetosheath– Gasdynamic Aspects

- The energy of the solar wind is dominated by the flow
- The theoretical way to deal with this is to treat the flow as gasdynamic and to neglect the magnetic field.
  - Back in the 1960's, John Spreiter and colleagues converted an existing numerical code to describe the bow shock and magnetosheath. The code had been developed to treat the flow around missiles.
  - They assumed an axially symmetric shape for the magnetopause.
- Since the solar wind is supersonic, it forms a shock as it encounters the Earth's magnetosphere and slows down
  - The collision mean free path of the solar wind is of the order of ~10^6 R_E, the thickness of the bow shock is of the order of the ion gyroradius (~1000 km)

Streamlines and Mach Lines

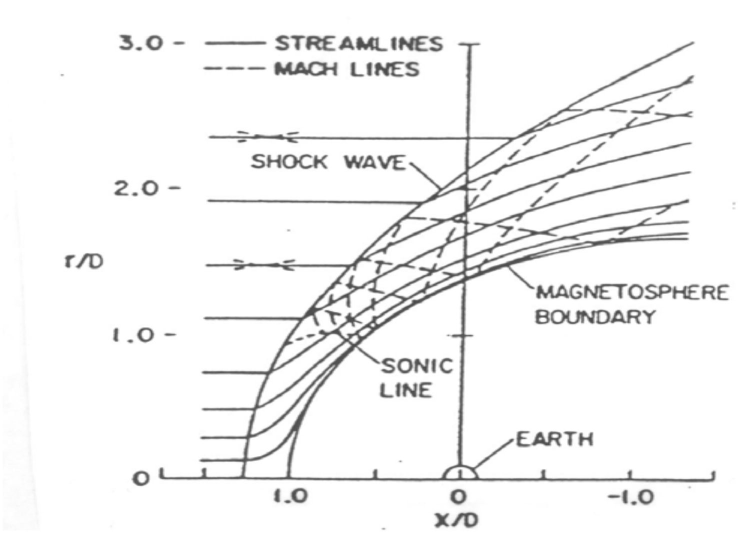

- This computation was for Mach number 8, $\gamma = 5/3$.
- The code computes the position of the shock self-consistently.
- Flow diverts around the obstacle, which is assumed impenetrable.
- The flow gets very slow right at the nose of the magnetosphere.
  - Flow accelerates away from there.
  - Flow becomes supersonic at the “sonic line.”

Density Distribution

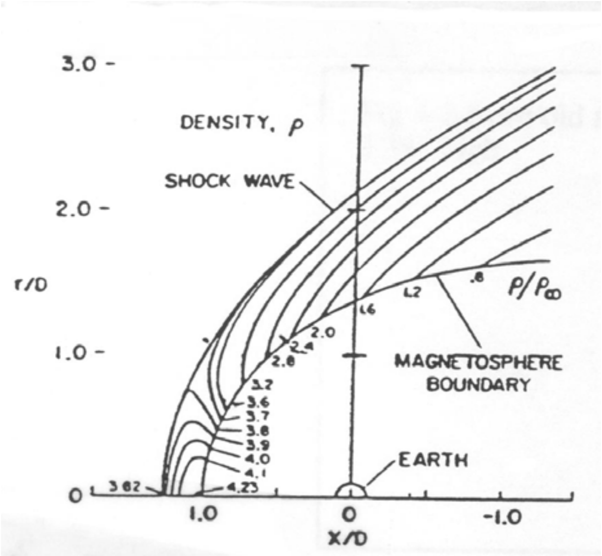

- Density:
  - For Mach number 8 and $\gamma = 5/3$, the model calculation indicates that the density jumps by a factor 3.82 across the shock.
  - Max density is at "subsolar point," 4.23 times solar wind density.
  - Density gradually decreases away from subsolar point.

Velocity and Temperature Distributions

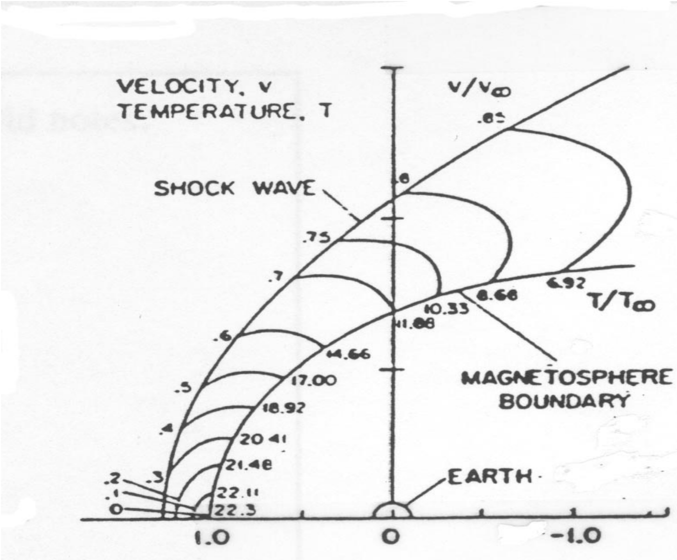

- Temperature decreases away from subsolar point
- Velocity increases away from that point.
- The contours for *T* and v are the same.

Magnetic Field Distribution

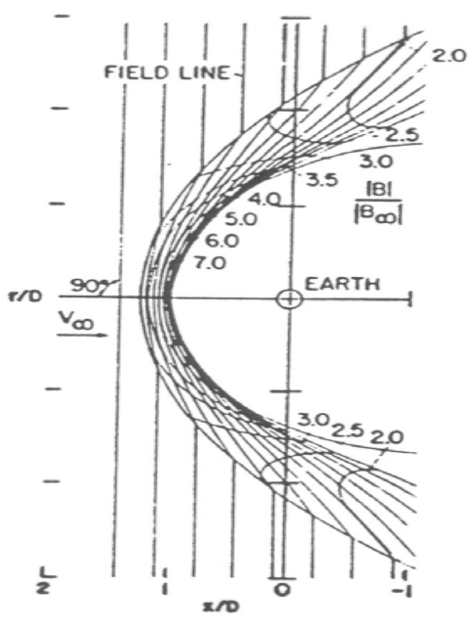

B ⊥ **v**

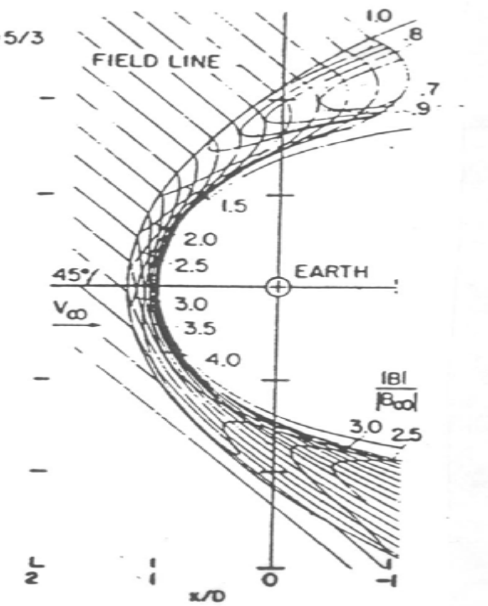

B at 45° to **v**

- Computed from assumption of frozen-in flux
- Note how magnetic field lines hang up on nose of magnetosphere
- B highest near subsolar point.
  - Zwan-Wolf effect
- In reality, the magnetosheath is very noisy

Effects of Mach Number

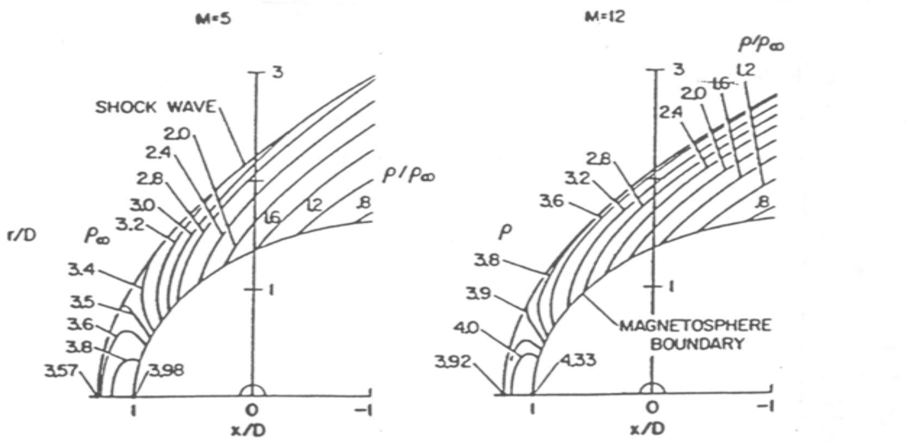

Effect of Mach number on density field for flow past the magnetosphere. γ = 5/3. From Spreiter et al. (1968), *ibid.*

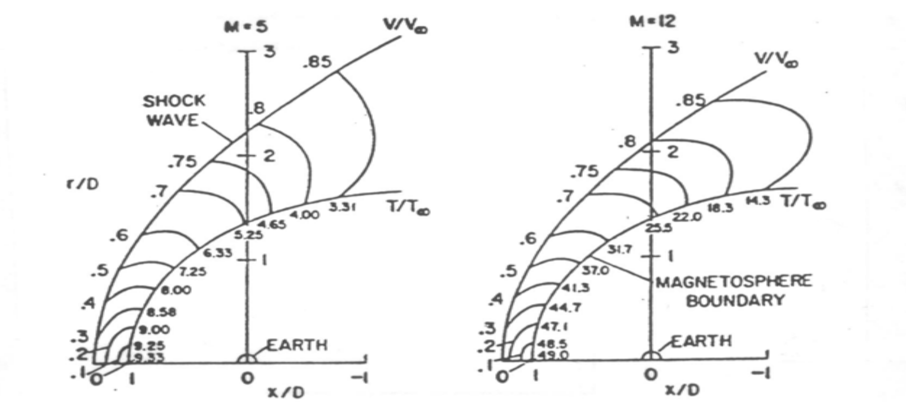

Effect of Mach number on velocity and temperature fields for flow past the magnetosphere, for γ = 5/3. From Spreiter et al. (1968), *ibid.*

Magnetic Cloud Events

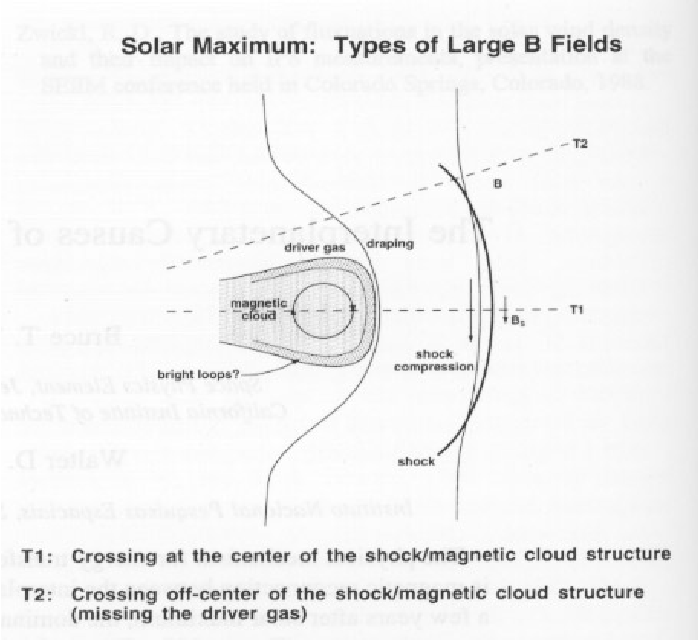

- Most very large magnetic storms on Earth are caused by magnetic clouds or "islands."
  - Strong organized magnetic field
  - Long period of northward field and long period of southward field.
    - Southward field causes storm

Magnetopause formation

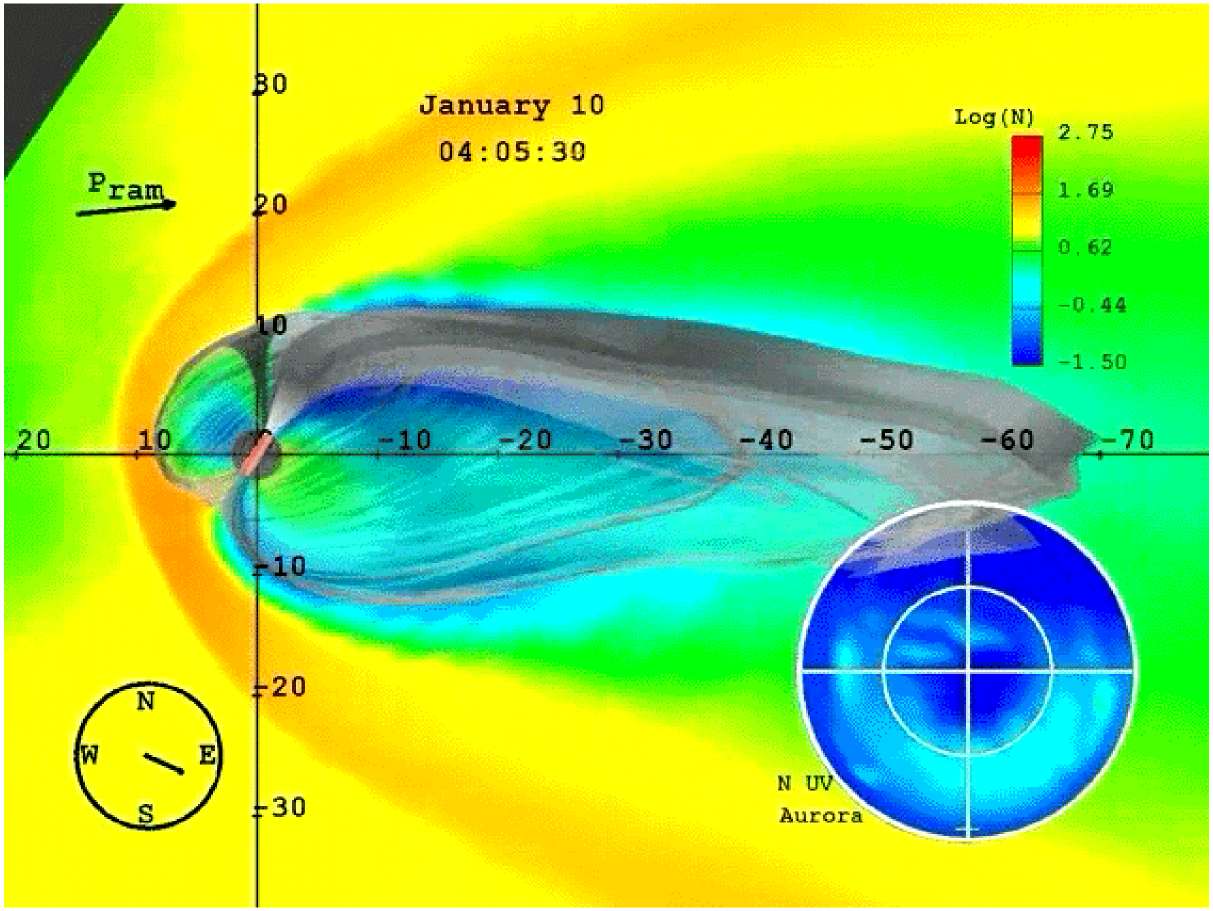

Snapshot from the LFM global magnetosphere code

Definition of “Magnetopause”

- An observer would want to define it in terms of something that is easy to observe, like a sharp jump in ‘something’.
- A theorist would want to define it in profound theoretical terms, such as the boundary between open and closed field lines.
  - However, that theorist’s definition doesn’t work - isn’t consistent with the established definition of the magnetosphere, which is the region dominated by Earth’s magnetic field.
  - Polar caps lie on open field lines, but at low altitudes they certainly lie in a region dominated by Earth’s field.
- We use an observational definition--a sharp change in the magnetic field.

Solar-Wind/Magnetosphere Coupling– Basic Physical Processes

Theories of an Ideal Magnetopause

Chapman-Ferraro Magnetopause

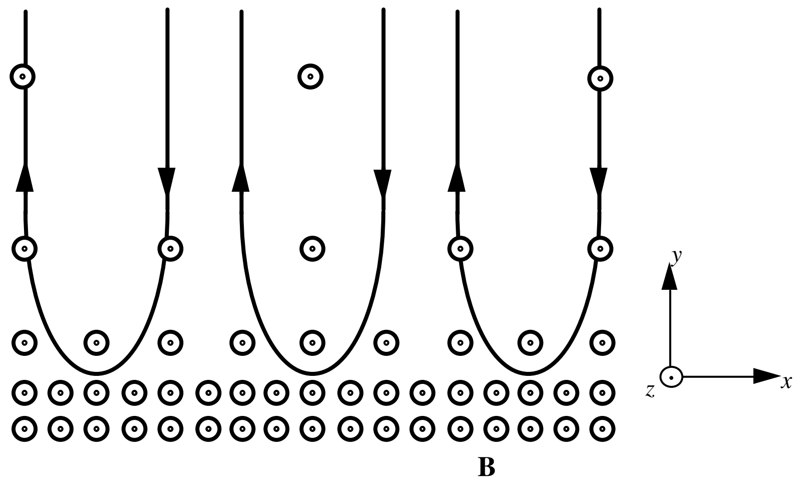

- 1D picture of the magnetopause, assuming unmagnetized solar wind $\mathbf{v} = -v_o\hat{\mathbf{e}}_y$
- Assume incident beam with density n_o,
- Magnetic field assumed parallel to z.
- Assume zero electric field.

Chapman-Ferraro-Type Magnetopause

- Solution for the magnetic field:

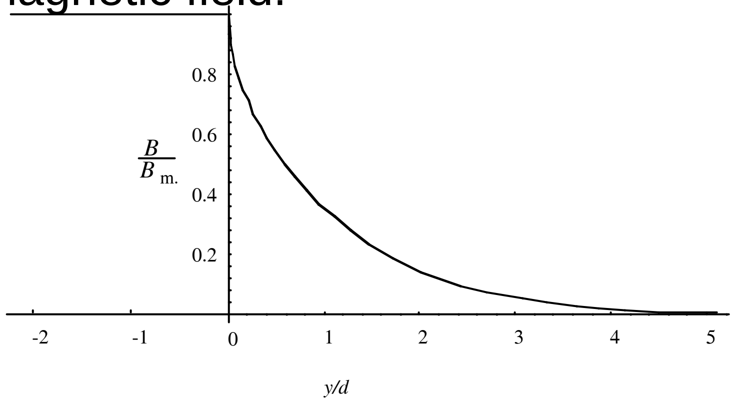

- The B-field scale length is related to the gyroradius inside the magnetosphere: $a_{cm} = \dfrac{mv_o}{qB_m} = \dfrac{d}{\sqrt{2}}$
- The momentum/area/time that the particles impart to the magnetic boundary is $$2n_o m v_o^2 = \frac{B_m^2}{2\mu_o}$$
  - Intuitively reasonable
- **The most fundamental conclusion of Chapman and Ferraro was that a boundary would form between the solar wind and magnetosphere, and that the solar wind would basically not penetrate to the space near Earth.**

Chapman-Ferraro-Type Magnetopause

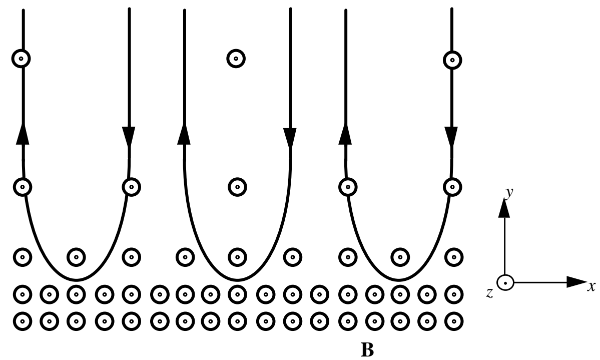

- One problem: charge imbalance:
  - Solar wind electrons presumably have the same density and flow velocity as the ions.
  - The electrons are much easier to turn around than the more massive ions
  - There is a negative charge layer above the positive charge layer
  - Order-of-magnitude estimate:

$$Surface\ \ charge\ \ density = \sigma_c \sim n_o q d$$

  - Potential difference across the charge separation layer:

$$\Delta V \sim \frac{\sigma_c d}{\varepsilon_o} \sim \frac{m_i}{2\mu_o \varepsilon_o q} \sim \frac{m_i c^2}{2q} \sim 500 \times 10^6\, V$$

Chapman-Ferraro-Type Magnetopause

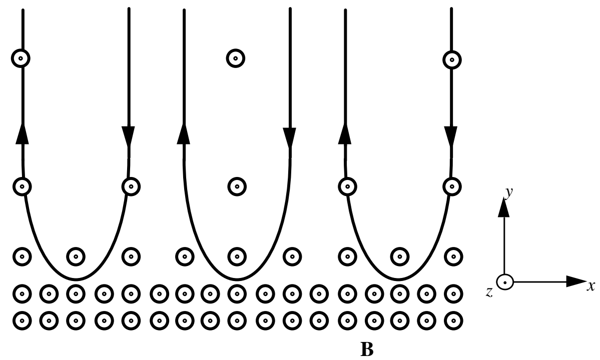

- Such a large potential drop can't be driven by particles ~ 1 keV
- Chapman and Ferraro realized this, and they enforced quasi-neutrality and calculated a self-consistent electric field.
  – They calculated a potential drop ~ $mv_o^2/2$
- Parker later pointed out that the magnetopause field lines connect to the conducting ionosphere.
  – If the charge density were maintained for a substantial time, then charges would flow up to and from the ionosphere, to eliminate the charge imbalance.

Models with a Self-Consistently Computed Magnetopause

- The first models with a self-consistently computed magnetopause were developed in the early 1960's.
- Assume

$$\mathbf{B}_\mathrm{o} = 0$$

where "o" means outside the magnetopause. Since $\nabla\cdot\mathbf{B}=0$, we require

$$\mathbf{B}_i \cdot \hat{\mathbf{n}} = 0$$

The total pressure in the magnetosheath just outside the magnetopause is estimated from the formula

$$p_o = k\rho_{sw}(\hat{\mathbf{n}} \cdot \mathbf{v}_{sw})^2$$

k=2 corresponds to the Chapman-Ferraro model. *k*=1 corresponds to particles sticking to the boundary. *k*=0.884 corresponds to the gasdynamic model with γ=5/3, *M*=8.

- The field just inside the magnetopause satisfies the pressure balance relation

$$\frac{\left|\hat{\mathbf{n}} \times \mathbf{B}_i\right|^2}{2\mu_o} = k\rho_{sw}(\hat{\mathbf{n}} \cdot \mathbf{v}_{sw})^2$$

Models with a Self-Consistently Computed Magnetopause

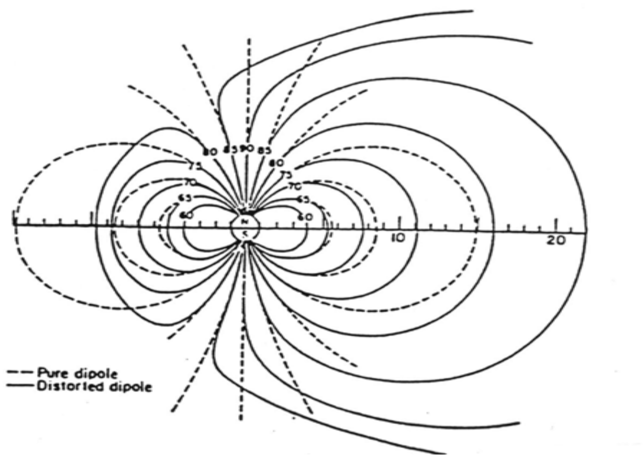

Mead (1964) model

- This model has a self-consistently computed magnetopause
  - No magnetotail (wasn't discovered until 1965)
  - Assumed $\nabla \times \mathbf{B} = 0$ inside the magnetopause.

Question

- In what direction is the magnetic field of the Chapman Ferraro currents?

Magnetospheric Current Systems

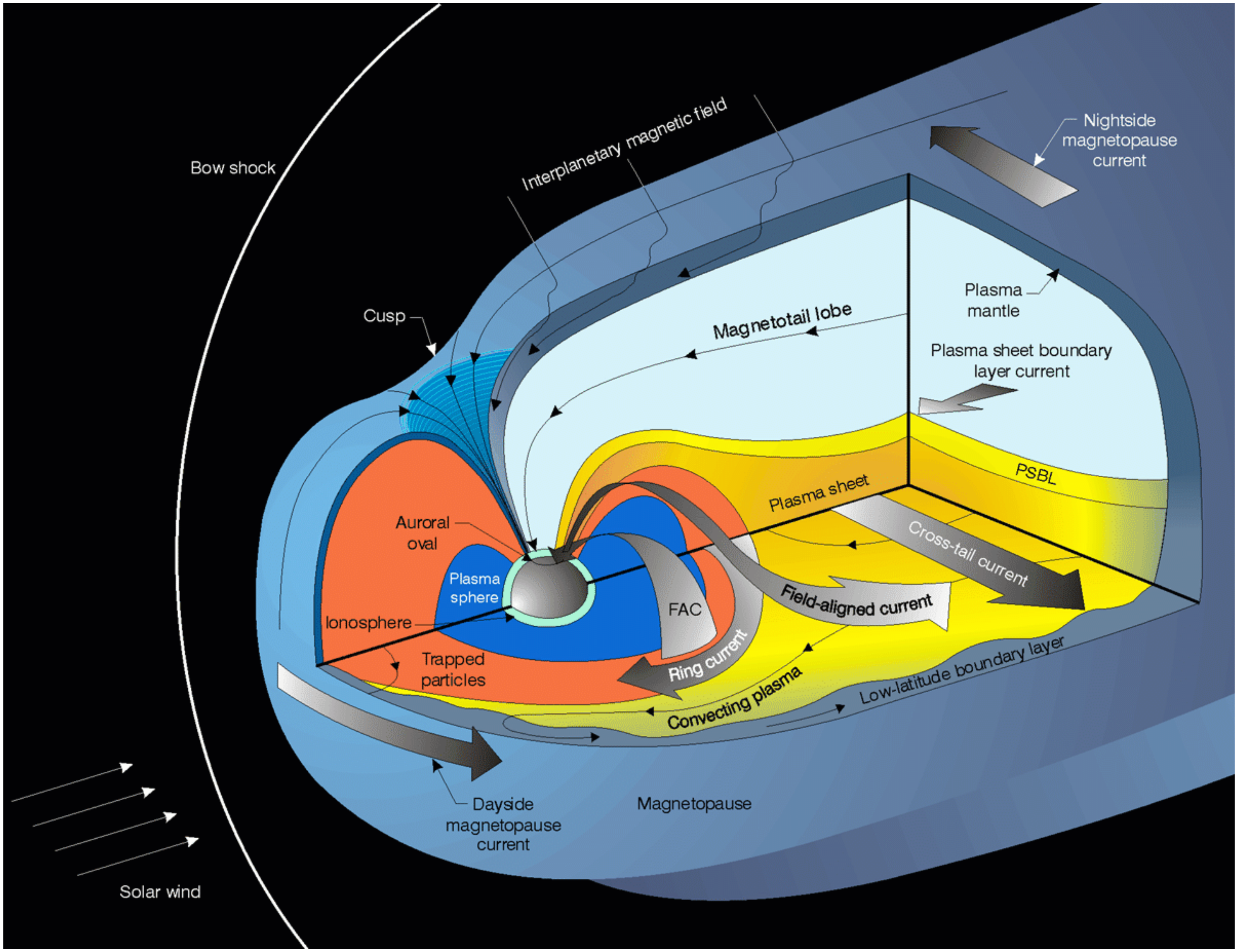

Early Self-Consistently Computed Magnetopauses

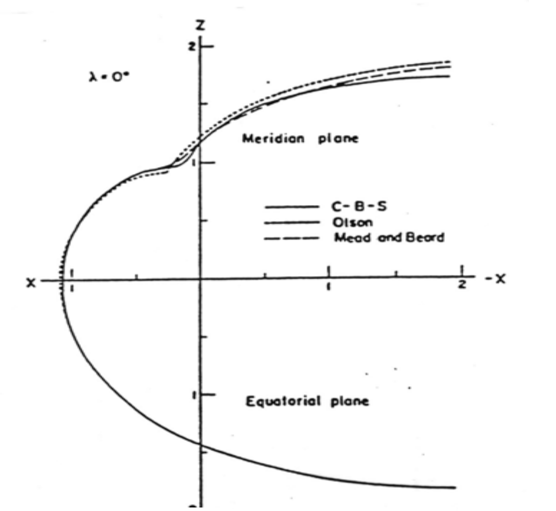

3 versions of Choe/Beard/Sullivan model in noon-midnight plane.

[Q: Why is there an indentation?]

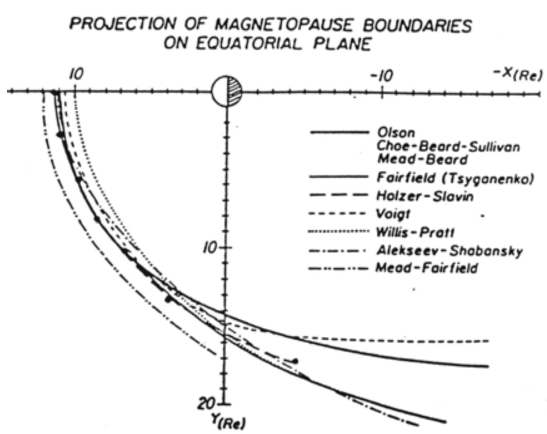

Model equatorial cross section

Dependence of Standoff Distance on Solar-Wind Parameters

- Define

$$B_i^{subsolar} = 2\,f\,B_{dipole}^{subsolar}$$

- The real magnetopause is between these two extremes.
- The results of the problem suggest that

$$1.0 \leq f \leq 1.5$$

- The pressure-balance relation becomes

$$k\rho_{sw}v_{sw}^2 = \frac{1}{2\mu_o}\left[2\,fB_o\left(\frac{R_E}{r_{so}}\right)^3\right]^2$$

- Solving for r_{so} gives

$$r_{so} = R_E\left(\frac{2f^2B_o^2}{k\mu_o\rho_{sw}v_{sw}^2}\right)^{1/6} = \frac{11.43\,R_E}{\left(\rho_{sw}v_{sw}^2\right)_{nPa}^{1/6}}\left(\frac{f}{1.16}\right)^{1/3}\left(\frac{0.885}{k}\right)^{1/6}$$

The best-estimate value for *f* is about 1.16 . A nominal solar wind (5 cm^{-3}, 400 km/s) corresponds to $\rho_{sw}v_{sw}^2$ = 1.34 nPa, which corresponds to r_{so}=10.9

Empirical Magnetopause Shapes

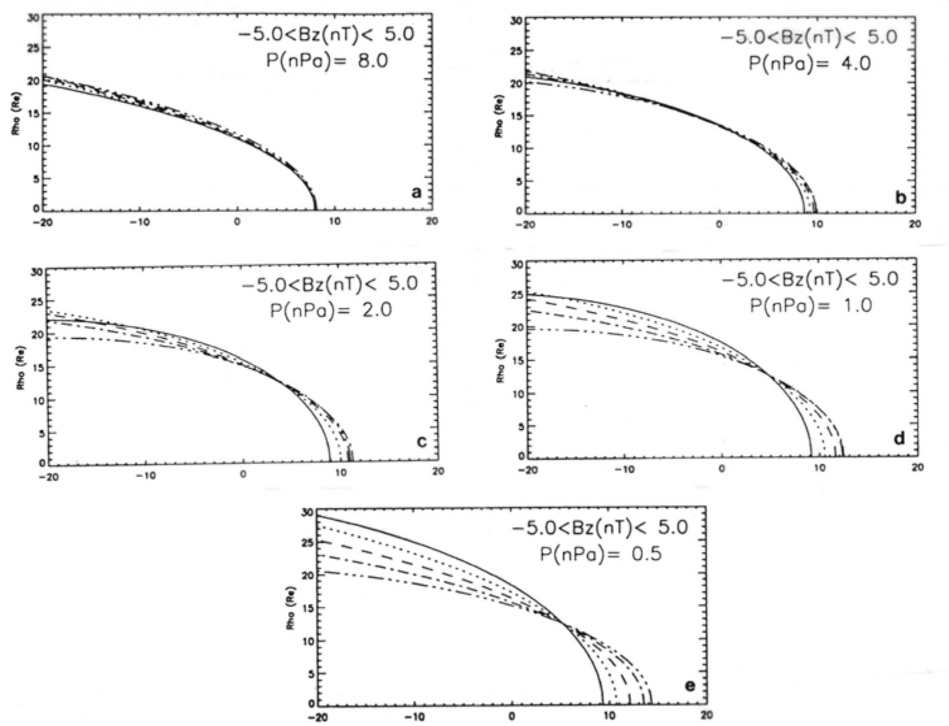

Average observed shape of magnetopause. Solid curve is -5 nT, dotted curve -2.5nT, dashed curve 0, dash-dot 2.5 nT, dash-dot-dot-dot 5.0 nT. Adapted from Roelof and Sibeck (JGR, 99, 8787, 1994)

- Note
  - Southward IMF moves magnetopause closer to Earth, strengthens tail lobes.
- Magnetopause position doesn't vary over a wide range (1/6 power)
  - Subsolar standoff distance is nearly always between 6.6 R_E and 14 R_E.

Features of the Observed Magnetic Field-ΔB

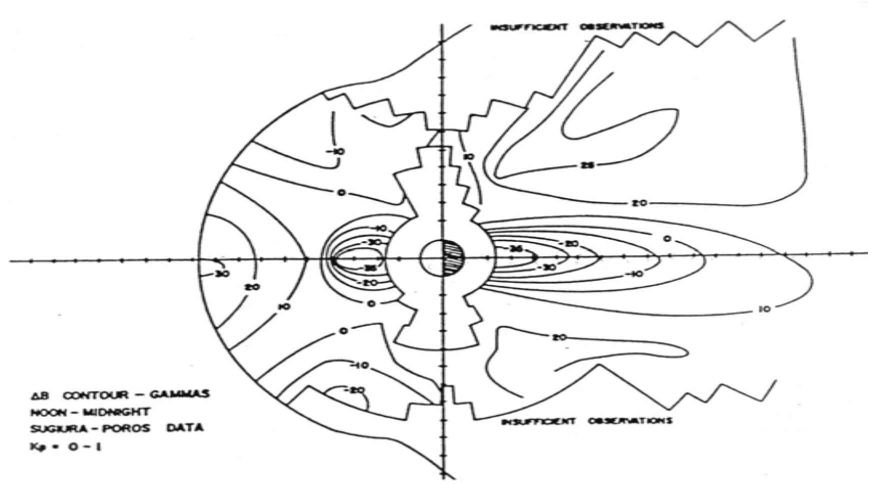

Sugiura and Poros plot of average ΔB for Kp=0 or 1.

$$\Delta B = \langle |\mathbf{B}_{observed}| \rangle - \langle |\mathbf{B}_{dipole}| \rangle$$

- Obvious features:
  - Compression of day side
  - Enhanced field in tail lobes
  - Depression in polar cusp
  - Depression of field near Earth and equatorial plane due to ring current

Decline of B_Z Downtail

- For $x > -20$,
  - B_z is nearly always positive on the flanks of the tail, occasionally negative near local midnight
  - The B_z distributions are much broader (indicating more variability)
    - Suggests both occasional x-lines earthward of -20.
    - Consistent with dipolarization of field in expansion phase.
- For $-45 < x < -20$,
  - $|B_z|$ smaller.
  - Sector doesn't matter much.

B_z Further Downtail

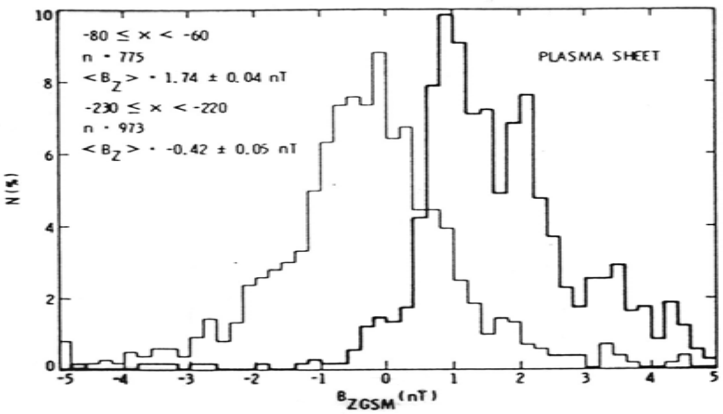

Histograms of z component of B in plasma sheet, from ISEE-3. From Siscoe et al.(1984).

- 60-80 R_E behind Earth, B_z is still usually positive.
- 225 R_E behind Earth, B_z is negative more than half the time.

Where Does Average B_z Turn Negative?

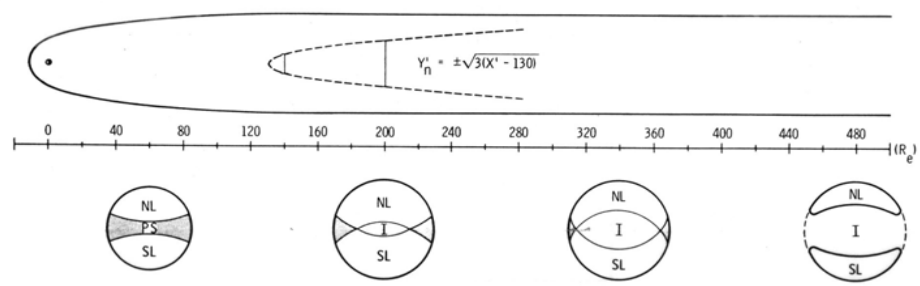

Location of separatrix between interplanetary field liens and closed field lines, from Slavin et al. (1985).

- Neutral line of average B_z:
  - ~ 130 R_E near local midnight
  - ~ 300 R_E on the flanks
- The "wake", which consists of field lines that are connected to the interplanetary medium on both "ends", becomes a larger and larger part of the tail as you go downstream.

Coupling processes

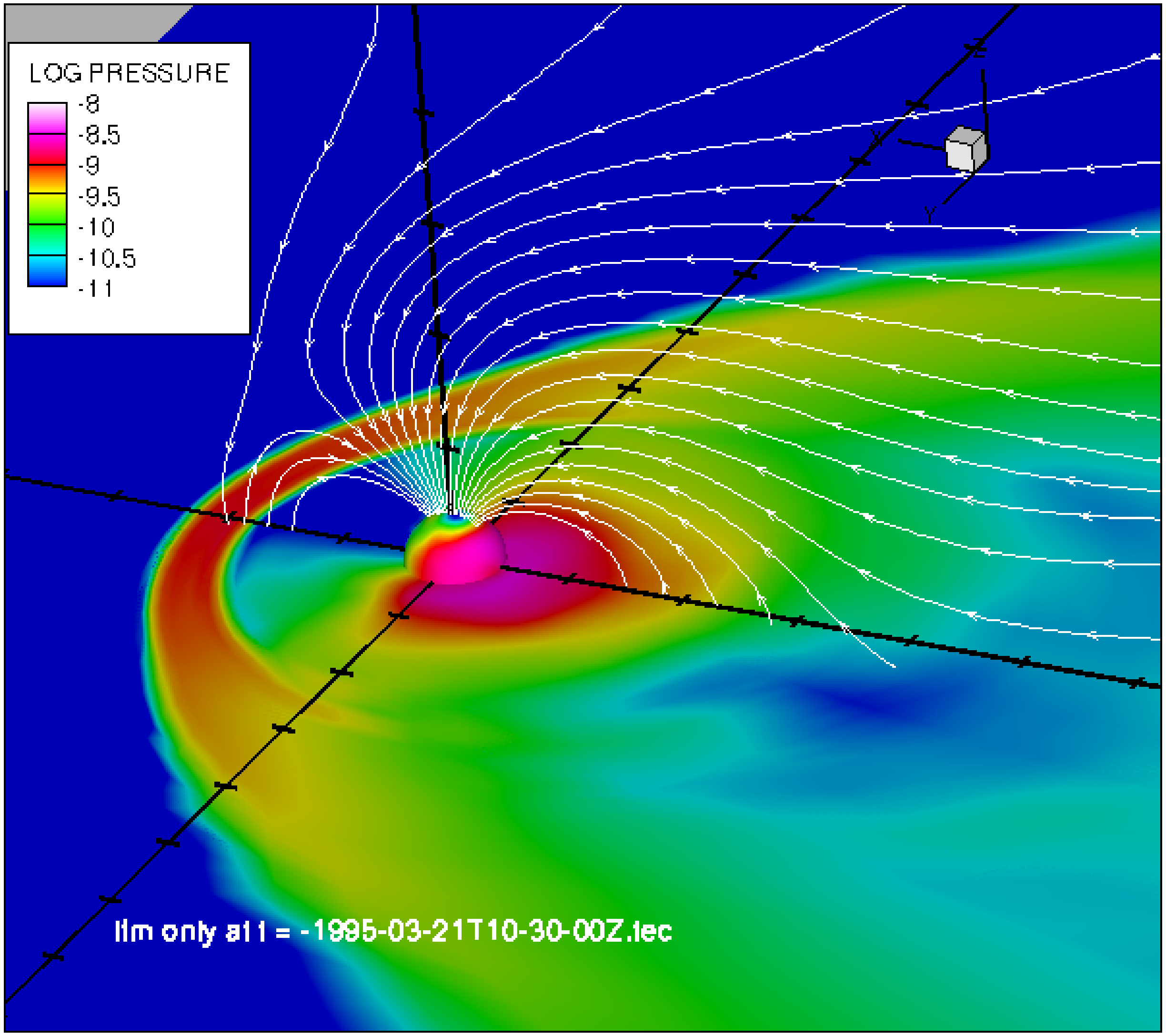

Basic Magnetospheric Convection

- Solar Wind Magnetosphere Coupling produces a system of plasma convection
  - Plasma in to the high latitude region connected to the outermost layers of the magnetosphere flow anti-sunward
  - Plasma in to the low latitude connected to the inner magnetosphere generally flow sunward
  - The presence of such convection suggest some form of drag or frictional force acting across the magnetopause

The Real Magnetopause apparently Isn't Ideal

- An ideal magnetopause – Chapman-Ferraro or tangential-discontinuity–has no mass flow across the boundary, no energy flux, no drag force.
- Some particles are observed in the magnetosphere that are clearly from the solar wind (He^{++}, for example).
- The long tail suggests that there is a substantial drag force.
- A southward turning of the interplanetary magnetic field (IMF) causes increased energy dissipation in the ionosphere
  - Clearly suggests that energy flows across the magnetopause into the magnetosphere.
- Therefore, we need to consider processes that transport particles, energy, or drag force across the magnetopause.

Transfer Processes at a Closed Magnetopause

- We will consider various closed-model transfer processes and try to estimate how efficient each is.
  - The crucial thing that we must explain is the rate of magnetospheric convection, the rate of circulation of plasma around the magnetosphere.
    - This turns out to be key--the observed rate of convection turns out to be harder to explain quantitatively than the observed rate of transfer of mass, momentum, and energy.
- How does one quantitatively characterize the rate of plasma circulation?
  - In ideal MHD, there is a simple answer: a voltage.

Potential Drop as a Measure of Convection

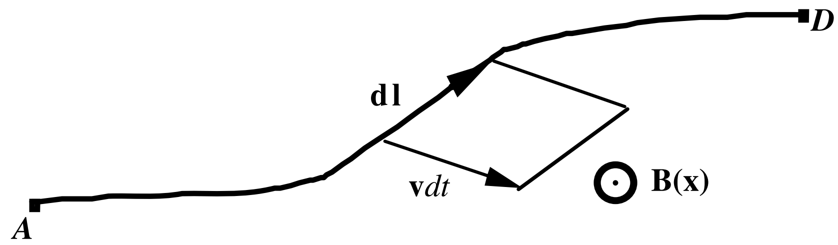

- How many field lines cross *AD* per unit time, assuming the perfect-conductivity relation

$$\mathbf{E}+\mathbf{v}\times\mathbf{B}=0$$

Consider field lines to move with the fluid elements that are locked to them.

$$\frac{d\Phi_M}{dt}=\frac{\int(\mathbf{v}dt)\times\mathbf{dl}\cdot\mathbf{B}}{dt}=-\int_A^D \boldsymbol{dl}\cdot\mathbf{v}\times\mathbf{B}=\int_A^D \boldsymbol{dl}\cdot\mathbf{E}$$

$$\frac{d\Phi_M}{dt}=-\int_A^D \boldsymbol{dl}\cdot\nabla\Phi=\Phi_A-\Phi_D$$

- Thus the number of magnetic flux tubes crossing *AD* per unit time is the potential difference between *A* and *D*.

Polar-Cap Potential Drop

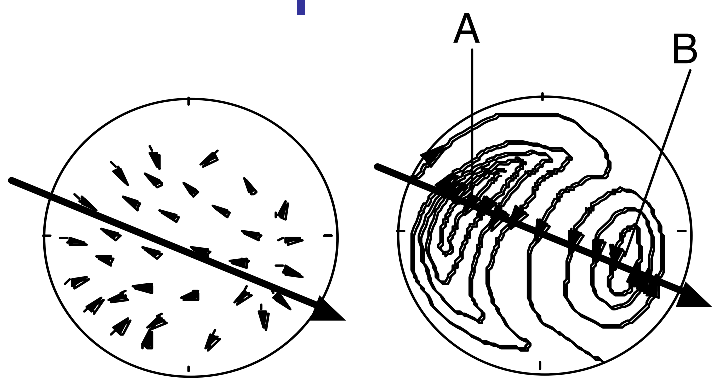

E

Equipotentials
and flow lines

- The potential drop across the high-latitude ionosphere can be measured by a polar-orbiting spacecraft.

$$\Phi_{pcp} = \int_{A}^{B} \mathbf{E} \cdot \boldsymbol{dl}$$

  – The polar cap potential drop Φ_{pcp} is measured routinely by satellites traversing the high-latitude ionosphere.

Polar-Cap Potential Drop

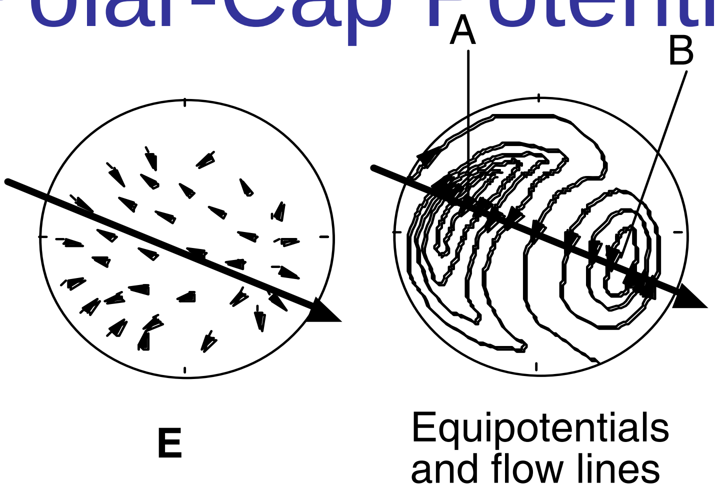

- Technical Problem: Satellite track doesn't usually cross either the max potential point *A* or the minimum potential point *B*.
  - Difference between max and min potential on satellite track is a lower limit on Φ_{pcp}.
  - Use only spacecraft in dawn-dusk orbit and estimate correction.
  - DMSP ion drift meter makes routine measurements of velocity perpendicular to the spacecraft track.
- Observed values:

$$20 \ kV \leq \Phi_{pcp} \leq 250 \ kV$$

$$\langle \Phi_{pcp} \rangle \approx 50 \ kV$$

Polar-Cap Potential Drop Driven by Viscous Interaction

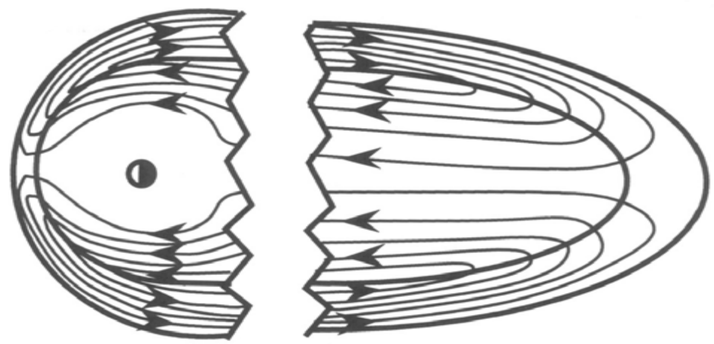

(adapted from Hill, 1983)

- Originally suggested by Axford and Hines (1961).
- Assume that the field lines are approximately equipotentials.
- If the average observed polar cap potential (50 keV)

$$h\langle B\rangle\langle v_{\perp}\rangle \sim 25 \quad kV$$

If<*B*>= 30 nT and <$v_{\wedge}$>=150 km/s (slightly less than half the solar-wind speed),

$$h \sim 6000 \quad km$$

Are there closed-model processes strong enough to create a closed-field-line boundary layer ~ 1 R_E thick?

Kelvin-Helmholtz Instability

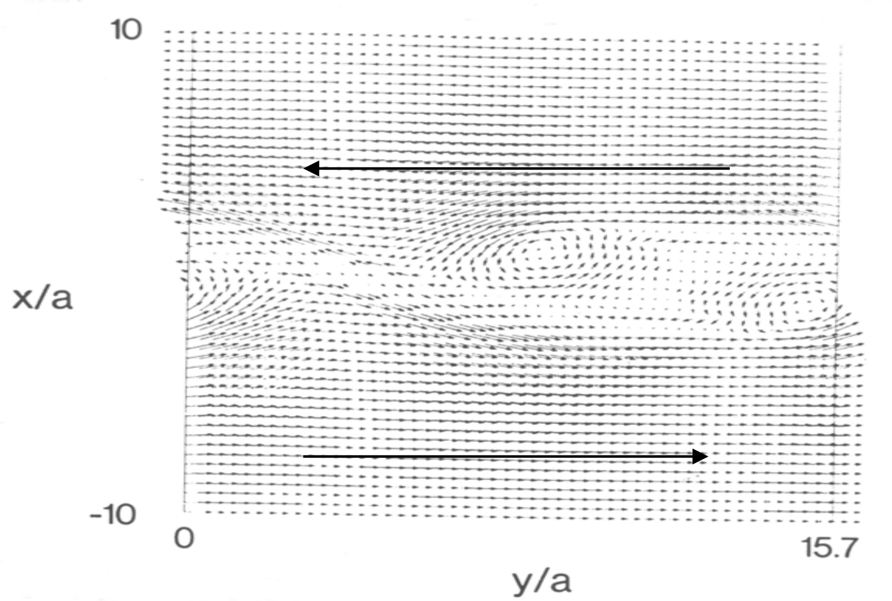

(Miura, 1984)

- Kelvin-Helmholtz instability is driven by a velocity shear
  - Ideal-MHD instability
  - Causes crinkling of the boundary
  - Velocity swirls
  - Tends to be stabilized by different magnetic field directions on the sides of the shear
  - In nonlinear phase, causes macroscopic friction
  - Computer simulations suggest 10-30 kV potential drop across magnetosphere (maybe enough to explain quiet-time convection)

Gradient/Curvature Drift Through Magnetopause

- The scale length L parallel to the boundary is ~ $10R_E$.
- To form a boundary 1 R_E thick about 20 R_E behind Earth, the average gradient-drift speed would have to be at least $<v_{\text{flow}}>/20$, and $<v_{\text{flow}}> \sim v_{\perp}$. Therefore, the ratio in is too small by almost 2 orders of magnitude.
- Conclusion: Gradient drift doesn't transport particles fast enough drive observed convection under average conditions.

Wave-Induced Diffusion Across the Magnetopause

- The magnetosheath has a lot of electromagnetic noise. Maybe that jiggles charged particles across field lines to form a thick boundary layer.
- **Bohm diffusion** (treatment from Hill, 1983):
  - To get an idea of how fast such wave-induced diffusion could possibly be, picture each wave-particle interaction as a collision. Assume the particle's velocity is completely randomized after each collision.
  - For the magnetopause boundary layer, put *kT*=200 eV, *B*=20 nT, and get a diffusion coefficient

$$\sqrt{\left\langle \Delta x^2 \right\rangle} \sim \sqrt{2 \times 600 \times 1200} \sim 1200 km$$

- This is ~ one-fifth the boundary-layer thickness required to drive the average observed convection.

Summary - closed transfer processes

- Optimistic estimate of Kelvin-Helmholtz provides < 40% of average drop
- Gradient drift provides ~10%
- Bohm diffusion (which is an upper limit) provides ~20%
- It’s even harder to explain the potential drop observed in storms, which is ~ 4 times average.
- These estimates are rough, but they suggest that these closed-field-line transfer processes are not the primary drivers of convection.

Low-Latitude Boundary Layer

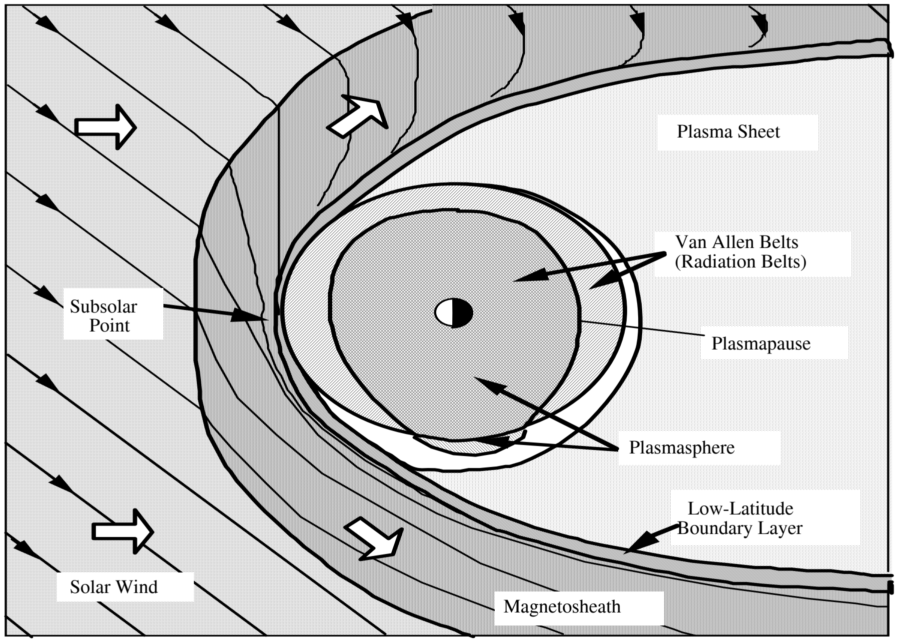

- Conventional wisdom is that much of the observed low-latitude boundary layer, which consists of antisunward-flowing plasma on the magnetopause, on northward-pointing magnetic fields, is driven by these closed-field-line transfer processes.
- These processes operate, but are not the primary drivers of convection.

Magnetic Reconnection

- Magnetic reconnection is the process whereby plasma ExB drifts across a magnetic separatrix, i.e., a surface that separates regions containing topologically different magnetic field lines
  - (Vasyliunas, *Rev. Geophys. Space Phys.*, *13*, 303, 1975)
  - In the original Dungey picture, reconnection occurs both on the dayside magnetopause and in the magnetotail.

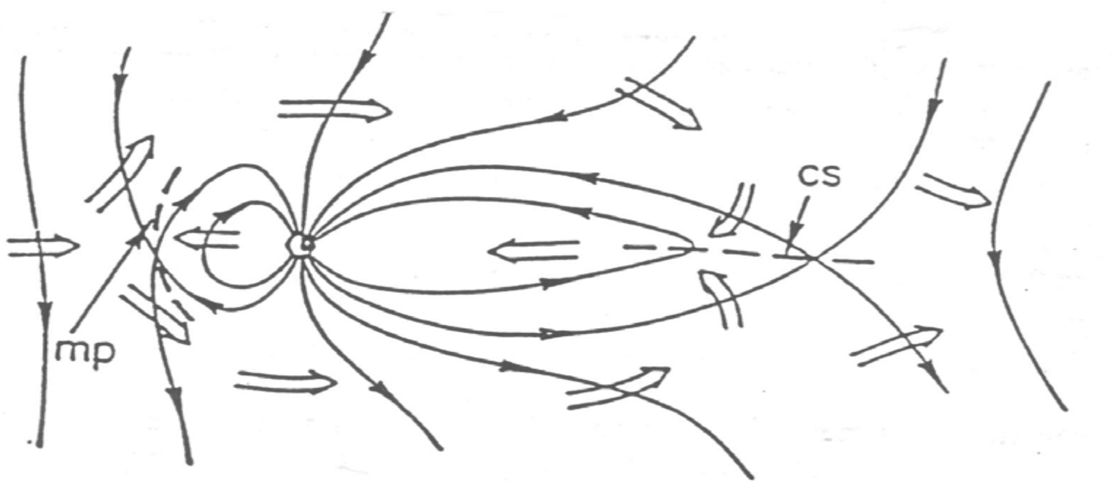

Empirical evidence

- Correlation of polar-cap potentia drop with VB_z (From Reiff and Luhmann (1986))

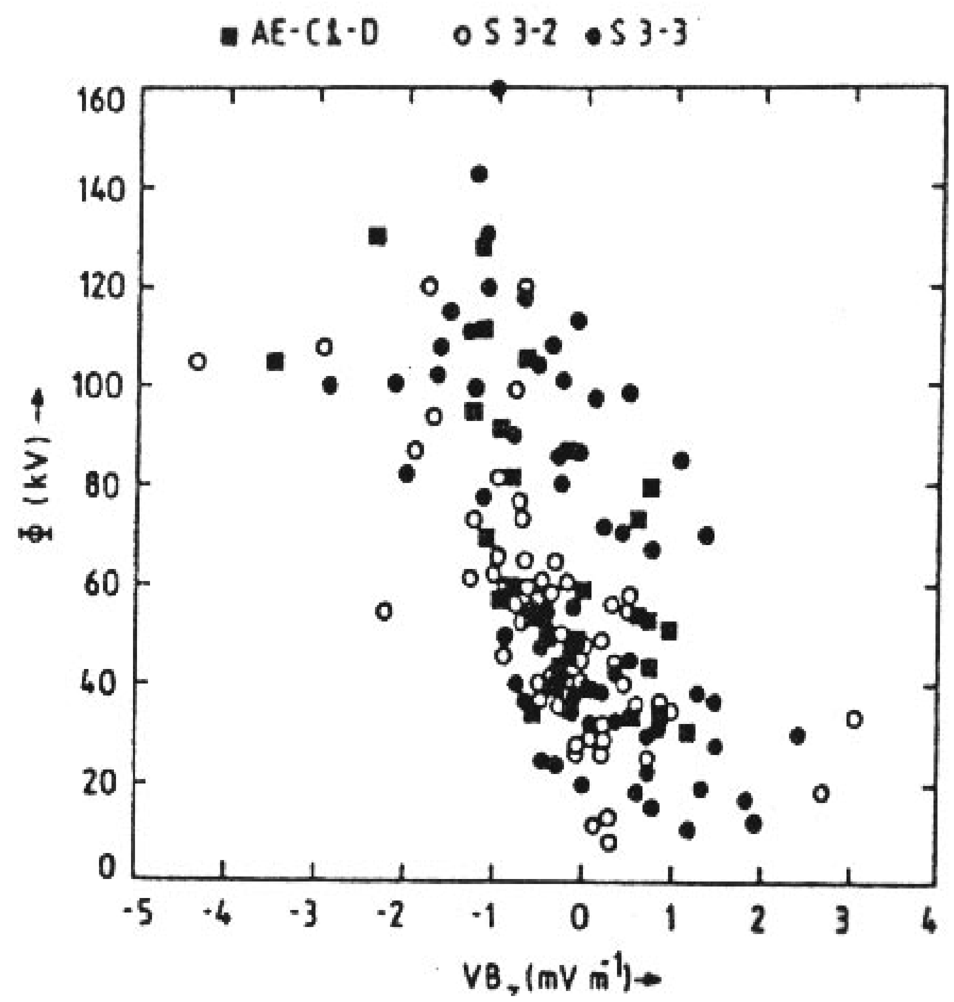

Summary - Open Magnetosphere

- The open model of the magnetosphere (Dungey, 1961) implied that convection would be strong for southward IMF
  - IMF is roughly anti-parallel to Earth’s dipole
  - Facilitates reconnection at dayside magnetopause
- That basic prediction has been strongly confirmed.
- This was substantial evidence that reconnection at the dayside magnetopause was the dominant driver of magnetospheric convection.

Polar Cap Saturation (Predicted by Hill, confirmed by simulations)

QuickTime™ and a
TIFF (Uncompressed) decompressor
are needed to see this picture.

QuickTime™ and a
TIFF (Uncompressed) decompressor
are needed to see this picture.

Effect of Ionospheric Conductance

QuickTime™ and a
TIFF (Uncompressed) decompressor
are needed to see this picture.

- The ionosphere plays an important role on determining the rate of convection on the ionosphere
    - The larger the conductance, the lower the convection rate

Where Does Average B_z Turn Negative?

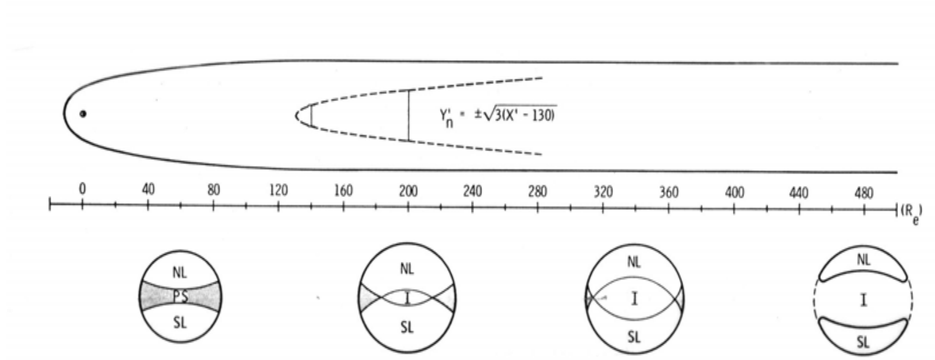

Location of separatrix between interplanetary field liens and closed field lines, from Slavin et al. (1985).

- Neutral line of average B_z:
  - ~ 130 R_E near local midnight
  - ~ 300 R_E on the flanks
- The “wake”, which consists of field lines that are connected to the interplanetary medium on both “ends”, becomes a larger and larger part of the tail as you go downstream.

Transfer of Particles into the Closed-Field-Line Region of the Magnetosphere

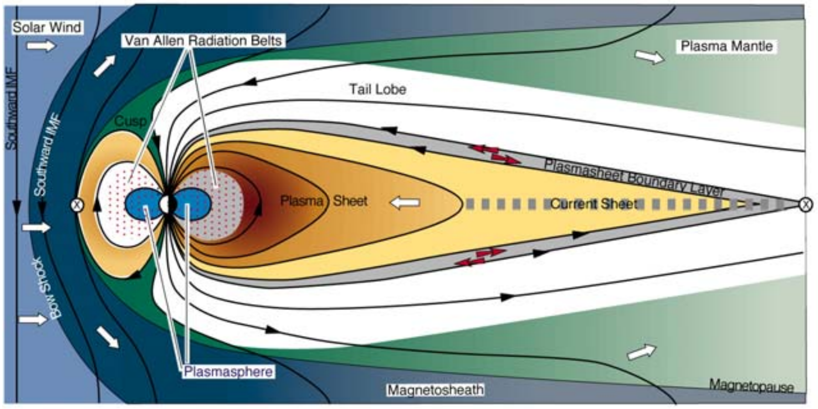

- Rate of earthward ion convection in the plasma sheet: $\Phi_{ions}^{pl.sh.} \sim (1cm^{-3})(50km/s)(8R_E)(30R_E) \sim 5\times10^{26}s^{-1}$
- Solar-wind particles incident on the front of the magnetosphere: $\Phi_{ions}^{solar\ \ wind} \sim (5cm^{-3})(400km/s)\pi(15R_E)^2 \sim 6\times10^{28}s^{-1}$
- Efficiency of particle penetration, assuming half the plasma sheet comes from the solar wind:

$$\eta_{ions} \sim \frac{\Phi_{ions}^{pl.sh.}}{2\Phi_{ions}^{solar\,wind}} \sim 0.004$$

Question

- Roughly what is the total amount of mass in the magnetosphere?
  - 2×10^{20} tons
  - 2×10^{10} tons
  - 20 tons
  - 2×10^{-12} tons

Transfer of Energy into the Inner Magnetosphere/Ionosphere

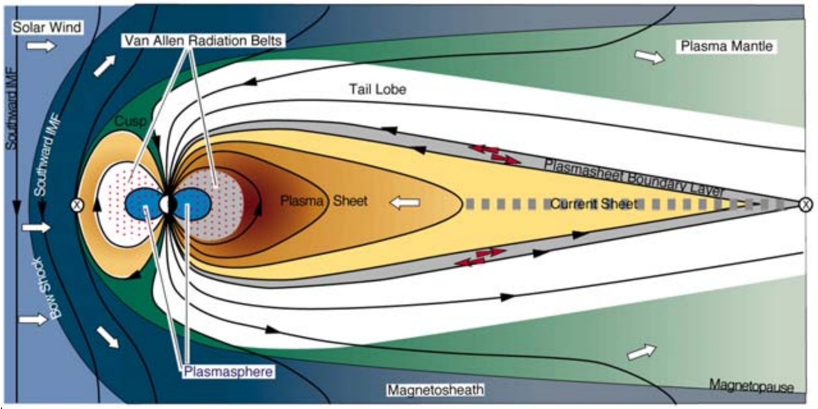

- Rate of Joule dissipation in the ionosphere:

$$\Phi_{energy}^{Joule\ \ heat} \sim (2\ \ hemispheres)(50,000 volts)(10^6 A) = 10^{11} watts$$

- Estimated total dissipation in inner magnetosphere and ionosphere: $$\Phi_{energy}^{diss.} \sim 2 \times 10^{11} watts$$

- Energy flux of solar wind times cross section of magnetosphere:

$$\Phi_{energy}^{sw} \sim \left(\frac{n_{sw} m_i v_{sw}^3}{2} \right) \pi \left(15 R_E \right)^2 \approx \frac{(5cm^{-3})}{2} m_H (400km/s)^3 \pi \left(15 R_E \right)^2 \sim 8 \times 10^{12} watts$$

- Efficiency with which energy penetrates to the magnetospheric interior and ionosphere:

$$\eta_{energy} = \frac{\Phi_{energy}^{dissipation}}{\Phi_{enery}^{sw}} \sim 0.025$$

Transfer Efficiencies for Fluid Quantities

- Much more mass enters the plasma mantle and immediately escapes down the tail. That mass wasn't counted in the efficiency.
- Much more energy also enters the magnetosphere in the plasma mantle and escapes down the tail but wasn't counted in the efficiency. The loss of solar wind kinetic energy is estimated as

$$\Phi_{energy}^{sw\ to\ tail} \sim \frac{(B_{lobe})^2}{\mu_o}(v_{sw})\pi(R_{tail})^2 / 2$$

$$\sim \frac{(20\times 10^{-9}\,nT)^2}{\mu_o}(4\times 10^5\,m/s)\pi(15\times 6.37\times 10^6\,m)^2 / 2 \sim 3\times 10^{12}\,watts$$

which is much larger than the energy dissipated in the ionosphere and magnetospheric interior.

Energy Input - Poynting Flux

- It can be shown that the rate of conversion to/from mechanical energy from/to magnetic energy is given by (Hill, 1982)

$$< \mathbf{j}.\mathbf{E} > = - < \nabla \cdot (\mathbf{E} \times \mathbf{B}) / \mu_0 >$$

- Where < > is a (sufficiently) long time average
- Basically, when
  - **j.E** > 0, magnetic energy is converted to flow energy
  - **j.E** < 0 flow energy is converted to magnetic energy

Example from Global MHD - BATSRUS - Southward IMF

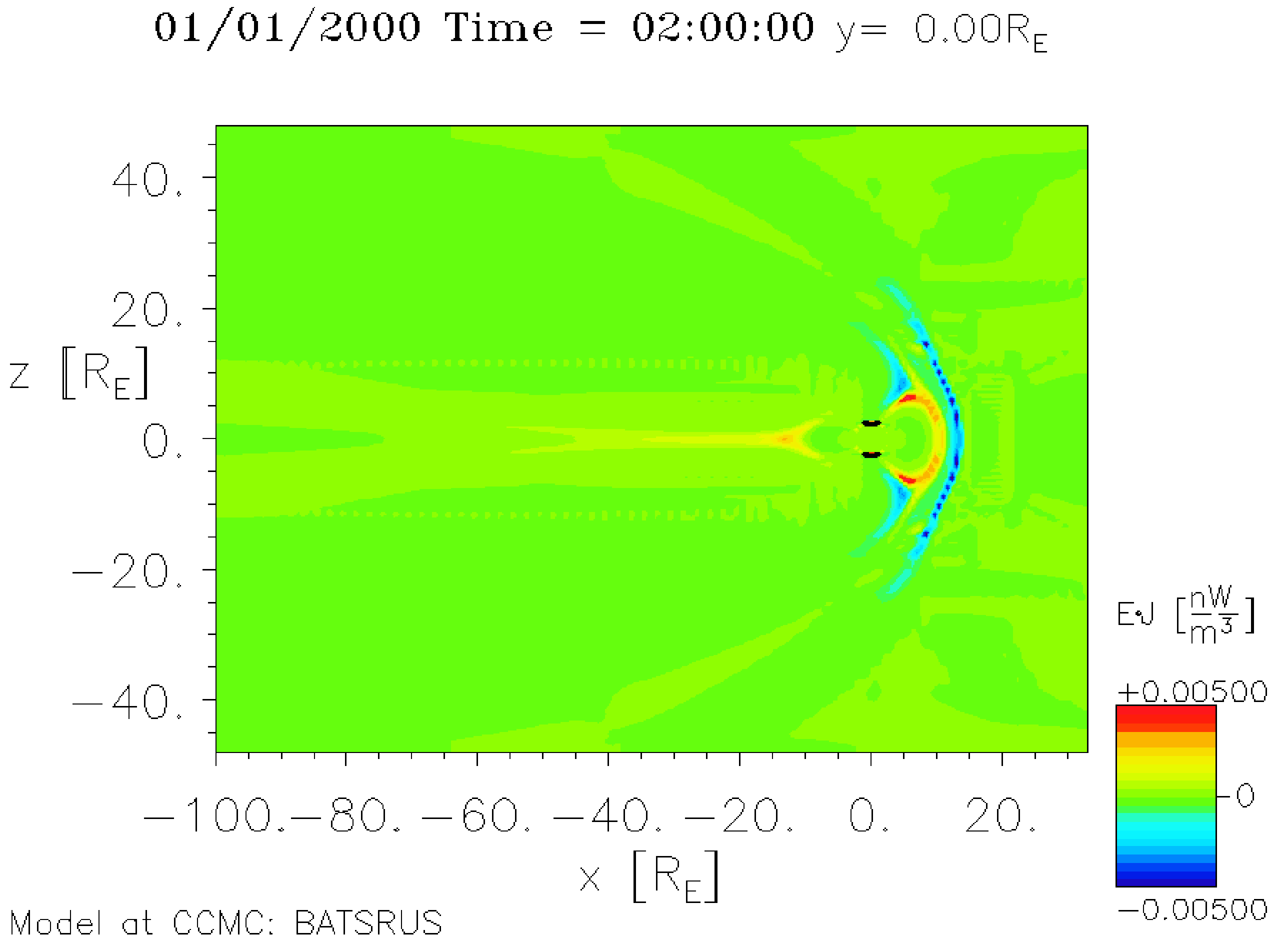

Example from Global MHD - BATSRUS -Northward IMF

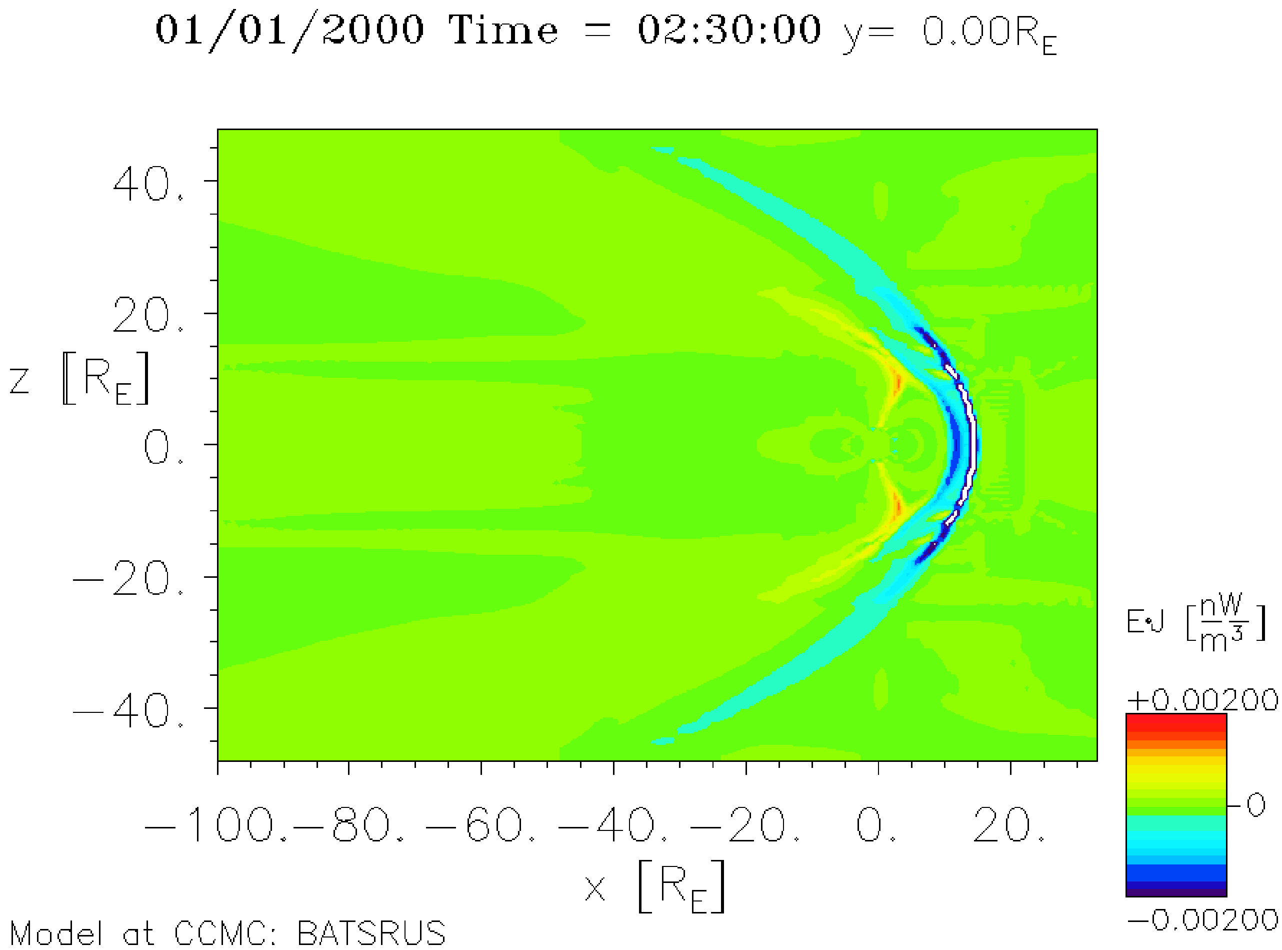

Example from Global MHD - OpenGGCM - Southward IMF

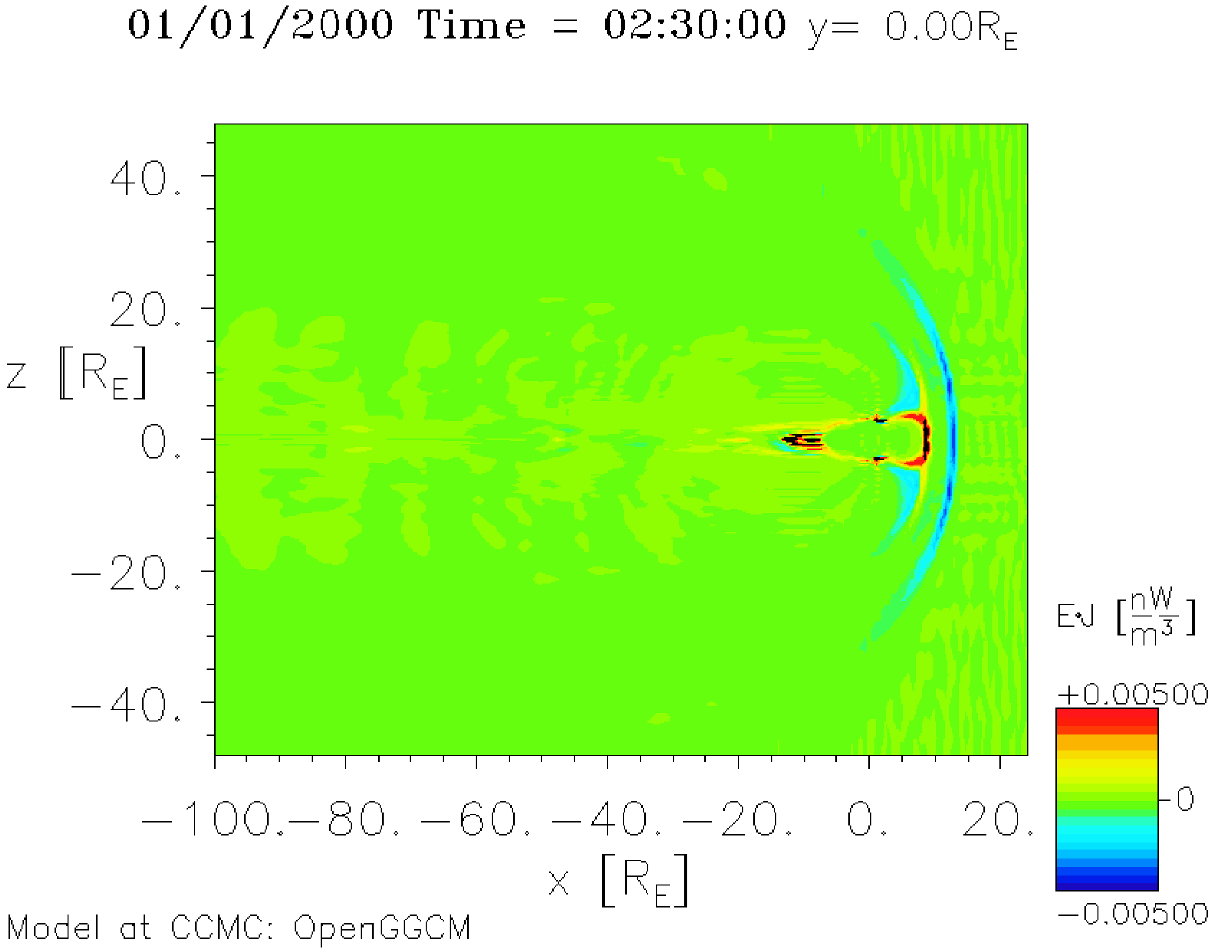

Examples from Global MHD - LFM - Southward IMF

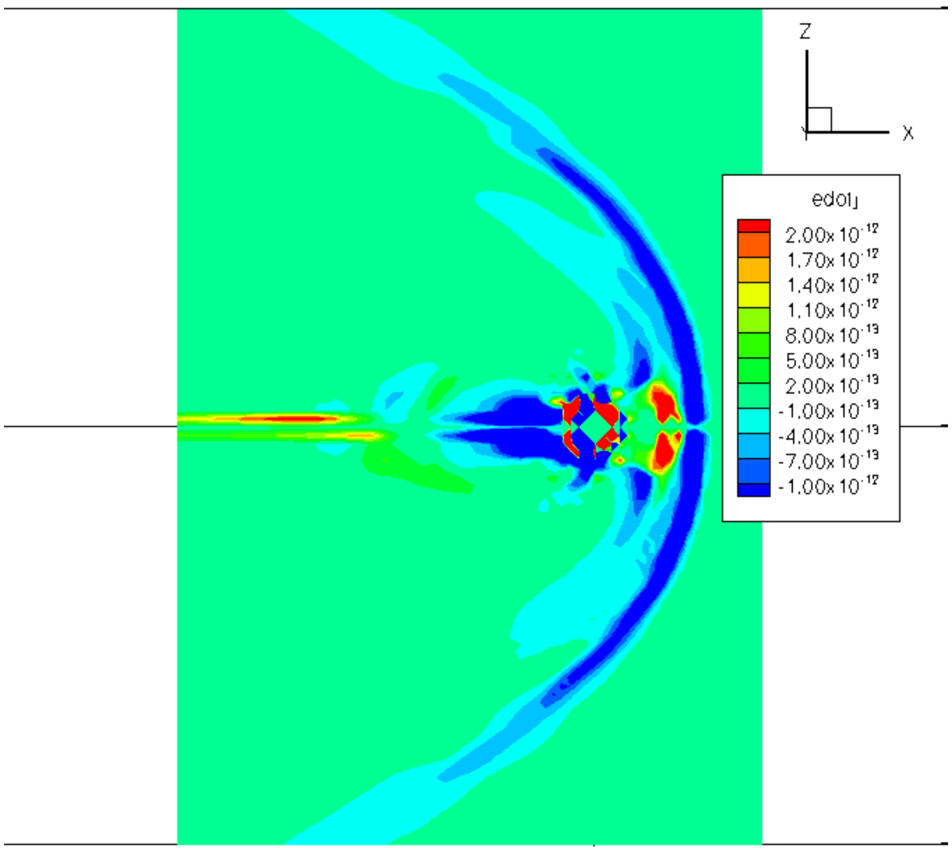

Momentum Coupling

- How does the force applied by solar wind manifest itself in the magnetosphere?
  - At the magnetopause, both normal and tangential forces are acting
  - The normal force is the solar wind ram pressure is

$$Ram\ force \sim ram\ \ pressure \times area\ \ presented\ \ to\ \ the\ \ SW$$

$$: \ (5\,cm^{-3})(1.67\times10^{-27}\,kg)(400\,km/s)^2\,\pi(15\,R_E)^2$$

$$\sim 4\times10^7\,N$$

Question

- Which is larger?
  - Solar wind dynamic pressure?
  - Solar radiation pressure?

Question

- Which is larger
  - Solar wind dynamic pressure? ~$2x10^{-9}$ Pa
  - Solar radiation pressure? ~$5x10^{-6}$ Pa

Question

- Which is larger
  - Solar wind dynamic force?
  - Solar radiation force?

Question

- Which is larger
  - – Solar wind dynamic force? ~2×10^7 N
  - – Solar radiation force? ~6×10^8 N

Comment on Forces

- With a force ~10^7 N, the ~200+ tons of plasma in the magnetosphere would be blown down the tail
- Ultimately the only mass able to hold off the force is the Earth itself [*Vasyliunas*, 2007]

Force of Chapman-Ferraro Current on the dipole

$$F_{CF} \approx \mu.\nabla B_{CF}$$

$$\approx (8 \times 10^{22})(1.5nT / R_E)$$

$$\approx 2 \times 10^{7} N$$

QuickTime™ and a
TIFF (Uncompressed) decompressor
are needed to see this picture.

Midgley and Davis, 1963)

From Siscoe and Siebert, JASTP 2006

From Global MHD

Siscoe and Siebert, 2006 got $2.4x10^{7}$N by integrating the momentum stress tensor over the volume.

QuickTime™ and a
TIFF (Uncompressed) decompressor
are needed to see this picture.

From Siscoe and Siebert, JASTP 2006

Changes of Chapman Ferraro and R-1 currents with increasing IMF Ey.

QuickTime™ and a
TIFF (Uncompressed) decompressor
are needed to see this picture.

From Siscoe and Siebert, JASTP 2006

Force

QuickTime™ and a
TIFF (Uncompressed) decompressor
are needed to see this picture.

Tan=positive, blue=negative

From Siscoe and Siebert, JASTP 2006

Tailward force on the thermosphere exceeds solar wind drag

QuickTime™ and a
TIFF (Uncompressed) decompressor
are needed to see this picture.

This was also noted by Hill, 1982 and discussed in detail by Vasyliunas, 2007

From Siscoe and Siebert, JASTP 2006

Comments on Transfer Efficiencies for Fluid Quantities

- Efficiency of momentum transfer:

$$\frac{Drag}{Ram\ force} \sim \frac{\dfrac{(20\,nT)^2}{2\mu_o}}{(5\,cm^{-3})(1.67\times10^{-27}\,kg)(400\,km/s)^2} \sim 0.12$$

where the numerator is an estimate of the tension force per unit area on the tail.

Penetration of Solar-Wind Magnetic Flux into Magnetotail

- Magnetic flux:
  - The magnetic flux in the polar cap (or tail lobes) is estimated as

$$\Phi_{Bn}^{pc} \sim \pi\left(\frac{15°}{57.296°}\right)^2 (6.27\times10^6 m)^2(.5\times10^{-4}T) \sim 4.4\times10^8 Wb$$

    These magnetospheric field lines are all connected to the solar wind and thus represent the effects of reconnection.
  - The magnetic flux that would thread through the region occupied by the magnetotail, if the magnetotail weren't there is estimated as $\Phi_{Bn}^{sw} \sim 40\times30\times300\times(6.37\times10^6 m)^2 \times(5\times10^{-9}T) \sim 2.4\times10^9 Wb$

    so the the efficiency with which the magnetic field gets across the tail magnetopause is estimated as

$$\eta_{Bn} \sim \frac{\Phi_{Bn}^{pc}}{\Phi_{Bn}^{sw}} \sim 0.18$$

Penetration of E_y into Magnetosphere in Times of Southward IMF

- The average observed polar cap potential drop in times of southward IMF is given roughly by

$$\Phi_{Ey}^{pc} \sim 80\, kV$$

- The average potential drop across a distance of 30 R_E (diameter of dayside magnetopause) would be

$$\Phi_{Etan}^{sw} \sim v_{sw} B_{sw} (30\, R_E) \sim (400\, km/s)(5\, nT)(30 \times 6.37 \times 10^6) \sim 382{,}000\, V$$

The implied efficiency is

$$\eta_{Etan} = \frac{\Phi_{Etan}^{pc}}{\Phi_{Etan}^{sw}} \sim 0.21$$

Summary Comments on Efficiency

- Only a small fraction (~1%) of the total particles and energy incident on the dayside magnetopause gets into the inner and middle magnetosphere, where there is sunward convection.
- A much larger fraction of the solar wind particles and momentum convect through the plasma mantle but never get deeply involved in the life of the magnetosphere.
- About 10-20% of the solar wind electric field penetrates, in times of southward IMF.

Global MHD models

- Global MHD models are now able to reproduce many of the global quantities discussed above
- However they often don't get the exact same results for the same inputs
  - Probably due to numerics such as resolution, numerical methods, etc
- While they seem to do a good job getting the gross scale physics correct, there is a lot of missing physics in the models
  - e.g, microphysics of reconnection, drift physics, etc
  - There has been efforts in the past few years to incorporate missing physics in the models

QuickTime™ and a
YUV420 codec decompressor
are needed to see this picture.

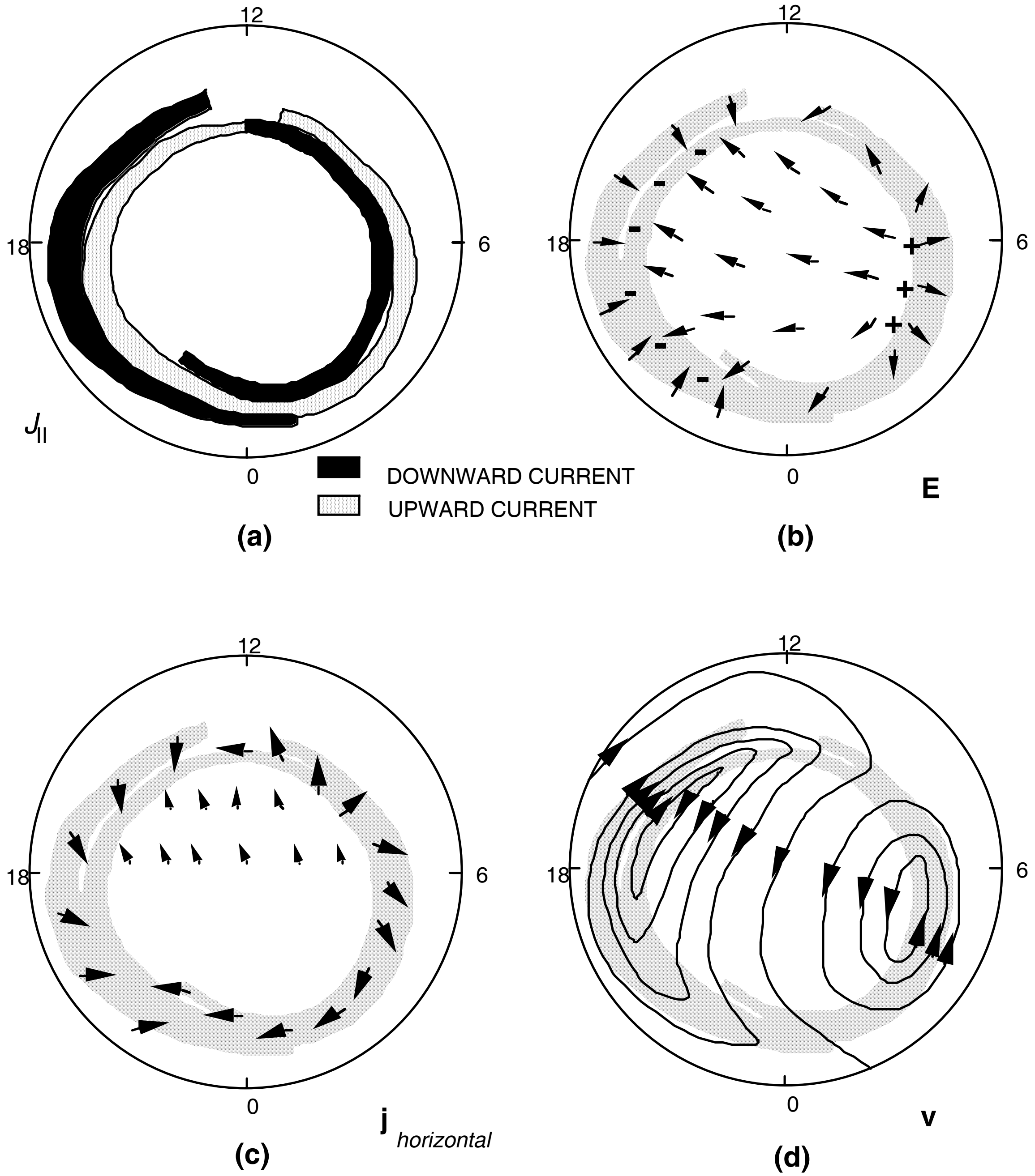
12
18
6
0
$J_{||}$
DOWNWARD CURRENT
UPWARD CURRENT
(a)
12
18
6
0
E
(b)
12
18
6
0
j horizontal
(c)
12
18
6
0
v
(d)

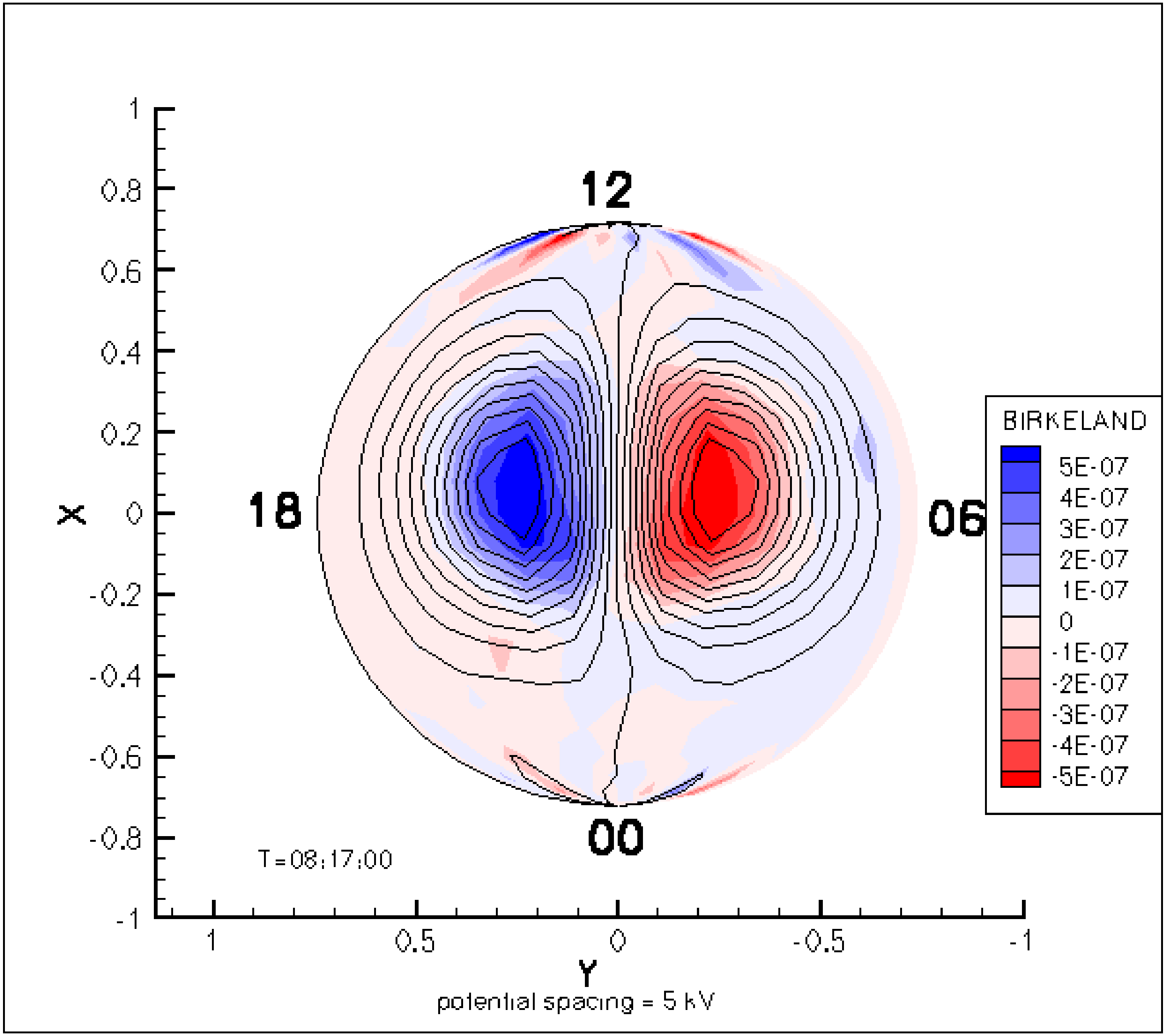

12
18
06
00
X
Y
1
0.8
0.6
0.4
0.2
0
-0.2
-0.4
-0.6
-0.8
-1
1
0.5
0
-0.5
-1
BIRKELAND
5E-07
4E-07
3E-07
2E-07
1E-07
0
-1E-07
-2E-07
-3E-07
-4E-07
-5E-07
T=08:17:00
potential spacing = 5 kV

Take home message: we think we understand a lot, but there are still a lot of fundamental unanswered questions, for example:

- To what extent is space weather (like surface weather) predictable, and to what extent is it (like surface weather) inherently unpredictable?
- Why are superthermal particles ubiquitous in space plasmas?
- Most of the solar system is occupied by collisionless plasma. Why are the positive ions, wherever you look, about 5-10 times hotter than the electrons?
- What is role of kinetic-scale processes in determining the large-scale structure of plasmas.?